11
Forward Dynamics of Flexible Multibody Systems

So far, several approaches to the solution of the kinematics and dynamics of multibody systems have been presented. It has been assumed in these approaches that all the bodies satisfy the rigid body condition. A body is assumed to be rigid if any pair of its material points do not present relative displacements. In practice, bodies suffer some degree of deformation; so this assumption does not hold in the strict sense. However, in the majority of the cases the relative displacements are so small that they do not affect the system's behavior. Therefore, they can be neglected without committing an appreciable error.

There are some important cases, however, in which deformation plays an important role. This is the case of lightweight spatial structures and manipulators or high-speed machinery. The dynamics of those systems is influenced by the deformation; thus the formulation of the preceding chapters cannot be applied. The complexity of the equations of motion considering deformation grows considerably. So does its size, since all the variables defining the deformation must also be considered.

In this chapter some of the methods that have been presented in the literature for the dynamics of flexible multibodies will be reviewed. Next a general method based on the moving frame approach will be described with natural coordinates that can be used when the elastic displacements are small. A formulation for beam-like elements based on the large displacement theory will be presented, and expressions for a nonlinear finite element that uses the same kind of Cartesian variables such as coordinates of points and components of unit vectors used in the previous chapters will be developed. Finally, some practical examples will be shown.

11.1 An Overview

In this section a quick overview will be given on some of the methods presented in the literature for the analysis of flexible multibody systems. Some of the work in the field was aimed at developing formulations suitable for particular

mechanisms such as the four-bar linkage or the crank and rocker mechanism. These approaches are not reviewed here, but the reader is referred to the papers by Lowen and Jandrasits (1972), Lowen and Chassapis (1986), Erdman and Sandor (1972), and Erdman and Sung (1986).

All the methods currently available may be divided into three main groups: a) the simplified methods based on elasto-dynamics, b) the methods based on defining the deformation with respect to a moving reference frame, and c) the methods based on defining the overall motion plus deformation with respect to an inertial frame.

In the simplified elasto-dynamic methods the deformation is considered uncoupled from the rigid body motion which is considered known by means of rigid body dynamics and is called the *nominal motion*. The main assumption is that the nominal motion induces deformations which are considered small, but that the deformations do not affect the nominal motion. This approach originally proposed by Winfrey (1971) was later expanded by Midha et al. (1978) and Sunada and Dubowsky (1981) to include inertial and centrifugal effects in the elastic equations. Naganathan and Soni (1987) proposed, for the case of open-chain flexible manipulators with independent coordinates (no constraint conditions), the use of elasto-dynamics with an iterative procedure that couples the elastic deformations with the nominal motion. For more general applications, the simplified approaches based on elasto-dynamics cannot be accepted since the coupling terms may strongly influence the solution. In such cases, one of the other two families of methods must be used.

The methods in the second group include all the nonlinear coupling terms in the formulation. Two kinds of variables are considered: first, the *rigid body variables*, that express the large nonlinear overall motion and characterize the moving frame of each body; second, the *deformation variables*, that express the state of deformation with respect to the moving frames. Both the relative displacements and the gradient of the displacements are assumed to be small, in order that the linear theory of elasticity holds. Some authors take as deformation variables the nodal variables resulting from a finite element discretization of the flexible body (Song and Haug (1980) and Serna and Bayo (1989)). Since this may lead to a large number of unknowns, one way of reducing the size of the problem consists in assuming that during the motion only a few modes will be excited and in taking the amplitude of such modes as unknowns. Shabana and Wehage (1983) used a popular substructuring technique called *component mode synthesis* (Hurty (1965)) to reduce the number of unknowns in each body. Other ways of selecting the most convenient assumed modes may be found in Craig (1981). Other authors (Book (1980), Kim and Haug (1988 and 1989), Changizi and Shabana (1988)) have developed recursive formulations that are based on the same approach for the definition of the deformation. A major advantage of the moving frame approach is that it makes use of the classical linear finite element theory to introduce either the nodal variables or the assumed mode shapes. Since there are a large number of reliable finite element codes well-known by engineers, this method has a special attractiveness. Some of the limitations of this

method have been pointed out by Kane et al. (1987), who showed that the moving frame approach with linear elasticity fails to consider the rotational stiffening effects that appear at very fast speeds of operation and which become important. As pointed out by Simo and Vu-Quoc (1987), second-order strain measures are necessary to capture these centrifugal stiffening effects through the geometric stiffness.

The third group encompasses a series of more recent methods, introduced first by Simo and Vu-Quoc (1986), that are based on the large rotation theory. Its main purpose is to develop nonlinear finite elements to be embedded in the multibody formalism. There is only one kind of variables, which are the global positions and orientations of the nodes referred either to an initial undeformed state (total Lagrangian formulation) or to a previously known state of deformation (updated Lagrangian formulation). These variables define at the same time the large translations, rotations, and deformations of the body. This method allows for the existence of arbitrarily large relative displacements and displacement gradients. However, since elastic constitutive relations are most commonly used, the assumption of small strains is often made. Unlike the moving frame approach, this method incorporates automatically the correct rotational stiffening terms and is well suited to study instabilities and buckling. Its main drawback is that the size of the problem cannot be reduced as in the moving frame approach. Therefore it is usually large. Furthermore, this formulation is limited to flexible bodies that can be modeled using beam and shell elements.

After considering this overview of all the methods available so far for the dynamic analysis of flexible multibodies, we are going to concentrate in this chapter: first, in the formulation of the classical approach of the moving frame with natural coordinates (Section 11.2) and secondly on a new formulation for beam-like elements based on the large displacement theory that is also based on the use of natural coordinates (Section 11.3). Note that both formulations are non-exclusive in the sense that one may be preferred over the other depending on the type of applications. Since both are based on the natural coordinates, they can perfectly coexist with the rigid-body formulation of the previous chapters, in a general purpose simulation package. In those cases in which the geometry is complicated and only small deformations are expected, the moving frame approach with assumed modes will be the best choice. Conversely, with simplified geometry and appearance of nonlinear effects the second approach will be the way to go.

11.2 The Classical Moving Frame Approach

In this section the moving frame method using the *natural coordinates* will be described (Vukasovic et al. (1993)). A complete formulation of the moving frame approach within the setting provided by the reference point coordinates has been described by Shabana (1989)). By means of the classical formulation, we use the natural coordinates of the body (or element) to unequivocally define the

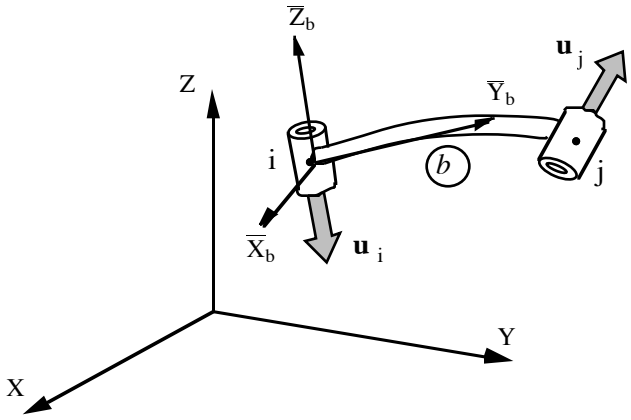

Figure 11.1. Flexible body with natural coordinates and the moving frame.

moving frame that moves with the large overall rigid body motion and to which the elastic deformation variables are referred. The natural coordinates of the body do not include relative translations or rotations and are subjected to the corresponding rigid body constraints. The formulation of the joint constraints is different than in the rigid body, because now points and vectors cannot be shared at the joints and the elastic deformations at those points need to be included.

11.2.1 Kinematics of a Flexible Body

Figure 11.1 shows a flexible body which will be denoted as *b* and which is defined by the two points *i* and *j* and by the two vectors $\mathbf{u}_i$ and $\mathbf{u}_j$. Note that points *i* and *j* are not material points but just two points chosen for the definition of the moving frame. We assume that $\mathbf{r}_j$–$\mathbf{r}_i$, $\mathbf{u}_i$, and $\mathbf{u}_j$ are not coplanar. If a body has more than two points and two vectors, the formulation can readily be modified to accommodate the additional coordinates by simply adding additional rigid body constraints (See Chapter 2).

Consider the moving reference frame ($\overline{X}_b$, $\overline{Y}_b$, $\overline{Z}_b$) attached to the body. Let $\mathbf{A}^b$ be the orthogonal rotation matrix that relates the inertial frame (X, Y, Z) to the body moving frame. We can write

$$\mathbf{X}^b = \mathbf{A}^b \, \overline{\mathbf{X}}^b \tag{11.1}$$

where $\mathbf{X}^b$ represents a (3×3) matrix whose columns are, respectively, $\mathbf{r}_j$–$\mathbf{r}_i$, $\mathbf{u}_i$, and $\mathbf{u}_j$. The upper bar denotes vectors referred to the moving frame. Similarly (See Chapter 4), $\overline{\mathbf{X}}^b$ is a (3×3) constant matrix, whose columns are $\overline{\mathbf{r}}_j$–$\overline{\mathbf{r}}_i$, $\overline{\mathbf{u}}_i$, and $\overline{\mathbf{u}}_j$. Matrix $\mathbf{A}^b$ can be obtained from equation (11.1) by simple inversion:

$$\mathbf{A}^b = \mathbf{X}^b \, (\overline{\mathbf{X}}^b)^{-1} \tag{11.2}$$

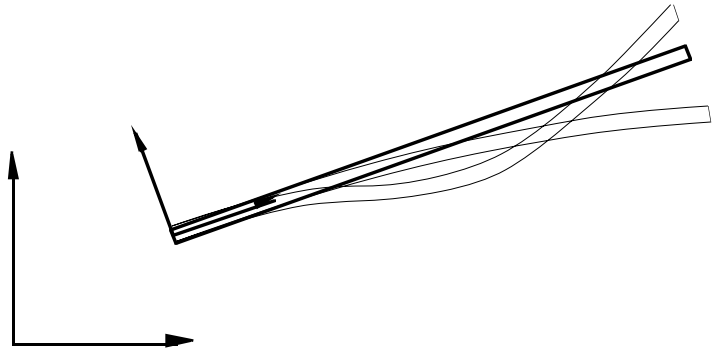

Figure 11.2. Cantilever modes of a beam-like flexible body.

Consider the body b and in it a material point P. Consider also a material segment through P, with its direction defined by a unit vector $\mathbf{u}_P$. The deformed position of P and $\mathbf{u}_P$ can be written as:

$$\mathbf{r}_P = \mathbf{r}_i + \mathbf{A}^b\ (\bar{\mathbf{r}}_P - \bar{\mathbf{r}}_i) + \mathbf{A}^b\ \delta\bar{\mathbf{r}}_P \tag{11.3}$$

$$\mathbf{u}_P = \mathbf{A}^b\ (\bar{\mathbf{u}}_P + \delta\bar{\mathbf{u}}_P) \tag{11.4}$$

where $\delta\bar{\mathbf{r}}_I$ represents the elastic displacement P, and $\delta\bar{\mathbf{u}}_I$ the elastic incremental rotation of $\mathbf{u}_P$, both expressed in the moving reference frame.

We can now proceed with the spatial discretization of the elastic displacement by defining a set of N_R Ritz vectors, such as finite elements or assumed modes for body b, namely $\bar{\boldsymbol{\phi}}^b_{Pk}$, $k = 1, \ldots, N_R$. These vectors are functions of the material coordinates $\bar{\mathbf{r}}_P$ of the point. The set $\bar{\boldsymbol{\phi}}^b_{Pk}$ contains the assumed displacement field corresponding to the assumed modes or finite elements with the rotations defined by the derivatives $\bar{\boldsymbol{\phi}}'^b_{Pk}$. Using this set of Ritz vectors, the displacements and rotations at point P can be expressed as:

$$\delta\bar{\mathbf{r}}_P = \sum_{k=1}^{N_R} \eta^b_k(t)\ \bar{\boldsymbol{\phi}}^b_{Pk} = \bar{\boldsymbol{\Phi}}^b_P\ \boldsymbol{\eta}^b \tag{11.5}$$

$$\delta\bar{\mathbf{u}}_P = \sum_{k=1}^{N_R} \eta^b_k(t)\ \bar{\boldsymbol{\phi}}'^b_{Pk} = \bar{\boldsymbol{\Phi}}'^b_P\ \boldsymbol{\eta}^b \tag{11.6}$$

where $\eta^b_k(t)$ are the time-dependent amplitude factors of the Ritz vectors (assumed modes or finite elements).

At this point, the analyst has two choices: a) consider a finite element model from which one can extract a reduced set of assumed modes using, for instance, component mode synthesis; or b) obtain a set of such modes experimentally through a vibration analyzer. Note that $\bar{\boldsymbol{\phi}}^b_{Pk}$ does not depend on time; thus it will not be differentiated. That the rigid body modes must also be eliminated from the

Ritz vectors, since the rigid body motion is already taken into account by the natural coordinates of the moving frame. One of several possible ways of imposing this condition is to select all the Ritz vectors with a clamped end at the origin of the moving frame. In this case, the moving frame attached to the elastic modes will be defined by ($\mathbf{r}_j$–$\mathbf{r}_i$) and $\mathbf{u}_i$. Note that $\mathbf{r}_j$ is not a material point of the elastic body. Figure 11.2 shows the two first cantilever modes for a beam-like body.

11.2.2 Derivation of the Kinetic Energy

In order to obtain the expression for the inertia forces we first derive the expression for the kinetic energy of the body *b* in the form

$$T^b = \frac{1}{2}\int_{v_b} \dot{\mathbf{r}}_P^{\mathrm{T}} \dot{\mathbf{r}}_P \, dm \tag{11.7}$$

Then, substituting equation (11.5) in (11.3) one can obtain

$$\mathbf{r}_P = \mathbf{r}_i + \mathbf{A}^b \left(\bar{\mathbf{r}}_P - \bar{\mathbf{r}}_i\right) + \mathbf{A}^b \, \bar{\boldsymbol{\Phi}}_P^b \, \boldsymbol{\eta}^b) \tag{11.8}$$

Substituting equations (4.49) and (4.50) into (11.8) one obtains

$$\mathbf{r}_P = \mathbf{C}_P^b \, \mathbf{q}^b + \mathbf{A}^b \, \bar{\boldsymbol{\Phi}}_P^b \, \boldsymbol{\eta}^b \tag{11.9}$$

where (See Chapter 4) $\mathbf{C}_P^b$ is a time invariant matrix that depends on the location of P, and $\mathbf{q}^b$ is the vector that contains the Cartesian coordinates of both the points *i* and *j* and the unit vectors $\mathbf{u}_i$ and $\mathbf{u}_j$. The velocity of P is obtained by the differentiation of equation (11.9):

$$\dot{\mathbf{r}}_P = \mathbf{C}_P^b \, \dot{\mathbf{q}}^b + \dot{\mathbf{A}}^b \, \bar{\boldsymbol{\Phi}}_P^b \, \boldsymbol{\eta}^b + \mathbf{A}^b \, \bar{\boldsymbol{\Phi}}_P^b \, \dot{\boldsymbol{\eta}}^b \tag{11.10}$$

Matrix $\dot{\mathbf{A}}^b$ may be expressed in terms of $\dot{\mathbf{q}}^b$ in the following manner: first, differentiate (11.2) to obtain

$$\dot{\mathbf{A}}^b = \dot{\mathbf{X}}^b \, (\bar{\mathbf{X}}^b)^{-1} \tag{11.11}$$

then, substitute this result into (11.10) to obtain

$$\dot{\mathbf{r}}_P = \mathbf{C}_P^b \, \dot{\mathbf{q}}^b + \dot{\mathbf{X}}^b \, (\bar{\mathbf{X}}^b)^{-1} \, \bar{\boldsymbol{\Phi}}_P^b \, \boldsymbol{\eta}^b + \mathbf{A}^b \, \bar{\boldsymbol{\Phi}}_P^b \, \dot{\boldsymbol{\eta}}^b \tag{11.12}$$

Now the second term on the RHS of (11.12) can be modified by defining a modal transformation matrix $\bar{\boldsymbol{\Psi}}_P^b$, such that

$$\bar{\boldsymbol{\Psi}}_P^b \equiv (\bar{\mathbf{X}}^b)^{-1} \, \bar{\boldsymbol{\Phi}}_P^b \tag{11.13}$$

The mentioned term may be expressed as

$$\dot{\mathbf{X}}^{\mathrm{b}}\,(\overline{\mathbf{X}}^{\mathrm{b}})^{-1}\,\overline{\mathbf{\Phi}}_{\mathrm{P}}^{\mathrm{b}}\,\boldsymbol{\eta}^{\mathrm{b}} = \dot{\mathbf{X}}^{\mathrm{b}}\,\overline{\mathbf{\Psi}}_{\mathrm{P}}^{\mathrm{b}}\,\boldsymbol{\eta}^{\mathrm{b}} = \dot{\mathbf{X}}^{\mathrm{b}}\sum_{k=1}^{NR}\bar{\mathbf{t}}_{\mathrm{Pk}}^{\mathrm{b}}\,\eta_{\mathrm{k}}^{\mathrm{b}} \tag{11.14}$$

where $\bar{\mathbf{t}}_{\mathrm{Pk}}^{\mathrm{b}}$ are the transformed modal vectors. The product of $\dot{\mathbf{X}}^{\mathrm{b}}\,\bar{\mathbf{t}}_{\mathrm{Pk}}^{\mathrm{b}}$ may be expressed as:

$$\begin{aligned}\dot{\mathbf{X}}^{\mathrm{b}}\,\bar{\mathbf{t}}_{\mathrm{Pk}}^{\mathrm{b}} &= \left[\dot{\mathbf{r}}_{\mathrm{j}} - \dot{\mathbf{r}}_{\mathrm{i}} \mid \dot{\mathbf{u}}_{\mathrm{i}} \mid \dot{\mathbf{u}}_{\mathrm{j}}\right]^{\mathrm{b}} \begin{Bmatrix}\bar{t}_1\\ \bar{t}_2\\ \bar{t}_3\end{Bmatrix}_{\mathrm{Pk}}^{\mathrm{b}} = \\ &= \left[-\bar{t}_1\,\mathbf{I}_3 \quad \bar{t}_1\,\mathbf{I}_3 \quad \bar{t}_2\,\mathbf{I}_3 \quad \bar{t}_3\,\mathbf{I}_3\right]_{\mathrm{Pk}}^{\mathrm{b}} \begin{Bmatrix}\dot{\mathbf{r}}_{\mathrm{i}}\\ \dot{\mathbf{r}}_{\mathrm{j}}\\ \dot{\mathbf{u}}_{\mathrm{i}}\\ \dot{\mathbf{u}}_{\mathrm{j}}\end{Bmatrix}^{\mathrm{b}} \equiv \mathbf{T}_{\mathrm{Pk}}^{\mathrm{b}}\,\dot{\mathbf{q}}^{\mathrm{b}}\end{aligned} \tag{11.15}$$

where $\mathbf{T}_{\mathrm{Pk}}^{\mathrm{b}}$ is a matrix that plays the same role of $\mathbf{C}_{\mathrm{P}}^{\mathrm{b}}$ but now is applied to the coordinates of the point P. Substituting (11.14) into (11.10) a final expression for the velocity of P is obtained:

$$\dot{\mathbf{r}}_{\mathrm{P}} = \mathbf{C}_{\mathrm{P}}^{\mathrm{b}}\,\dot{\mathbf{q}}^{\mathrm{b}} + \sum_{k=1}^{NR}\eta_{\mathrm{k}}^{\mathrm{b}}\,\mathbf{T}_{\mathrm{Pk}}^{\mathrm{b}}\,\dot{\mathbf{q}}^{\mathrm{b}} + \mathbf{A}^{\mathrm{b}}\,\overline{\mathbf{\Phi}}_{\mathrm{P}}^{\mathrm{b}}\,\dot{\boldsymbol{\eta}}^{\mathrm{b}} \tag{11.16}$$

Finally, by substituting (11.18) into the expression of the kinetic energy (11.7), we arrive at the following final expression:

$$T^{b} = \frac{1}{2}\left\{\dot{\mathbf{q}}^{\mathrm{bT}}\;\dot{\boldsymbol{\eta}}^{\mathrm{T}}\right\}\begin{bmatrix}\mathbf{M}_{\mathrm{rr}}^{\mathrm{b}} & \mathbf{M}_{\mathrm{rf}}^{\mathrm{b}}\\ \mathbf{M}_{\mathrm{fr}}^{\mathrm{b}} & \mathbf{M}_{\mathrm{ff}}^{\mathrm{b}}\end{bmatrix}\begin{Bmatrix}\dot{\mathbf{q}}^{\mathrm{b}}\\ \dot{\boldsymbol{\eta}}^{\mathrm{b}}\end{Bmatrix} \tag{11.17}$$

where

$$\begin{aligned}\mathbf{M}_{\mathrm{rr}}^{\mathrm{b}} = \int_{Vol}\mathbf{C}_{\mathrm{P}}^{\mathrm{bT}}\,\mathbf{C}_{\mathrm{P}}^{\mathrm{b}}\,dm + \sum_{k=1}^{NR}\eta_{\mathrm{k}}^{\mathrm{b}}\int_{Vol}(\mathbf{C}_{\mathrm{P}}^{\mathrm{bT}}\,\mathbf{T}_{\mathrm{Pk}} + \mathbf{T}_{\mathrm{Pk}}^{\mathrm{T}}\,\mathbf{C}_{\mathrm{P}}^{\mathrm{b}})\,dm + \\ + \sum_{k=1}^{NR}\sum_{l=1}^{NR}\eta_{\mathrm{k}}^{\mathrm{b}}\,\eta_{\mathrm{l}}^{\mathrm{b}}\int_{Vol}\mathbf{T}_{\mathrm{Pk}}^{\mathrm{bT}}\,\mathbf{T}_{\mathrm{Pl}}^{\mathrm{b}}\,dm\end{aligned} \tag{11.18}$$

$$\mathbf{M}_{\mathrm{rf}}^{\mathrm{b}} = \int_{Vol}\mathbf{C}_{\mathrm{P}}^{\mathrm{bT}}\,\mathbf{A}^{\mathrm{b}}\,\overline{\mathbf{\Phi}}_{\mathrm{P}}^{\mathrm{b}}\,dm + \sum_{k=1}^{NR}\eta_{\mathrm{k}}^{\mathrm{b}}\int_{Vol}\mathbf{T}_{\mathrm{Pk}}^{\mathrm{T}}\,\mathbf{A}^{\mathrm{b}}\,\overline{\mathbf{\Phi}}_{\mathrm{P}}^{\mathrm{b}}\,dm \tag{11.19}$$

$$\mathbf{M}_{\mathrm{ff}}^{\mathrm{b}} = \int_{Vol}\overline{\mathbf{\Phi}}_{\mathrm{P}}^{\mathrm{bT}}\,\mathbf{A}^{\mathrm{bT}}\,\mathbf{A}^{\mathrm{b}}\,\overline{\mathbf{\Phi}}_{\mathrm{P}}^{\mathrm{b}}\,dm = \int_{Vol}\overline{\mathbf{\Phi}}_{\mathrm{P}}^{\mathrm{bT}}\,\overline{\mathbf{\Phi}}_{\mathrm{P}}^{\mathrm{b}}\,dm \tag{11.20}$$

The sub indexes $(\text{-})_{\mathrm{r}}$ and $(\text{-})_{\mathrm{t}}$ have been used to differentiate the terms corresponding to the rigid body motion characterized by $\dot{\mathbf{q}}^{\mathrm{b}}$ from those that correspond to elastic deformations characterized by $\dot{\boldsymbol{\eta}}$. It may be observed from those expres-

sions how both $\dot{\mathbf{q}}^{\mathrm{b}}$ and $\dot{\boldsymbol{\eta}}$ are coupled in two different ways: a) through the coupling matrices $\mathbf{M}^{\mathrm{b}}_{\mathrm{rf}}$ y $\mathbf{M}^{\mathrm{b}}_{\mathrm{fr}}$; b) and by means of the $\boldsymbol{\eta}$ dependent terms that are included in $\mathbf{M}^{\mathrm{b}}_{\mathrm{rr}}$ and which appear in equation (11.20). The first term on the RHS of equation (11.20) coincides with the mass matrix of the rigid element as developed in Section 4.2. The second term contains a summation term that is linear in the elastic deformations $\boldsymbol{\eta}$. The last term contains a double summation that depends on the square of the elastic deformations. If one is consistent with the assumption of small deformations, these square terms may be neglected for all practical purposes. However, the second linear term in $\boldsymbol{\eta}$ may not be neglected as a general rule. Only after a careful comparison of the magnitude of these terms with those corresponding to the rigid case, may they be neglected. It may be finally observed that $\mathbf{M}^{\mathrm{b}}_{\mathrm{ff}}$ does not depend either on the deformation or the rigid body coordinates. It is the constant mass matrix usually considered in structural dynamics (Craig (1981)).

Equation (11.18) contains integrals that are independent of both position as well as time. These can be computed only once prior to the numerical integration of the equations of motion. The integral of the first term of this equation was seen in detail in Section 4.2. In the following exercise, it will be shown how to compute in an efficient manner the second term of this equation.

Example 11.1

Assuming that the Ritz vectors have been computed using finite elements, develop a procedure to integrate

$$\int_{Vb} (\mathbf{C}^{\mathrm{bT}}_{\mathrm{P}} \mathbf{T}_{\mathrm{Pk}} + \mathbf{T}^{\mathrm{T}}_{\mathrm{Pk}} \mathbf{C}^{\mathrm{b}}_{\mathrm{P}})\, dm \tag{i}$$

Solution: Recall that the expressions for $\mathbf{C}^{\mathrm{b}}_{\mathrm{P}}$ and $\mathbf{T}^{\mathrm{b}}_{\mathrm{Pk}}$ are:

$$\mathbf{T}^{\mathrm{b}}_{\mathrm{Pk}} = \left[\; -\bar{t}_1\, \mathbf{I}_3 \;|\; \bar{t}_1\, \mathbf{I}_3 \;|\; \bar{t}_2\, \mathbf{I}_3 \;|\; \bar{t}_3\, \mathbf{I}_3 \; \right] \tag{ii}$$

$$\mathbf{C}^{\mathrm{b}}_{\mathrm{P}} = \left[(1-\bar{c}_1)\, \mathbf{I}_3 \;|\; \bar{c}_1\, \mathbf{I}_3 \;|\; \bar{c}_2\, \mathbf{I}_3 \;|\; \bar{c}_3\, \mathbf{I}_3 \; \right] \tag{iii}$$

where the vectors $\bar{\mathbf{t}}^{\mathrm{b}}_{\mathrm{Pk}}$ y $\mathbf{c}_{\mathrm{P}}$ have been defined in equations (11.16) and (4.55), respectively, as:

$$\bar{\mathbf{t}}^{\mathrm{b}}_{\mathrm{Pk}} = \left[\overline{\mathbf{X}}^{\mathrm{b}} \right]^{-1} \bar{\boldsymbol{\phi}}^{\mathrm{b}}_{\mathrm{Pk}} \tag{iv}$$

$$\mathbf{c}_{\mathrm{P}} = \left[\overline{\mathbf{X}}^{\mathrm{b}} \right]^{-1} (\bar{\mathbf{r}}_{\mathrm{P}} - \bar{\mathbf{r}}_{\mathrm{i}}) \tag{v}$$

It becomes obvious that one does not need to integrate the matrix products as they appear in (i). It is sufficient to compute the following integral

$$\int_{Vb} \mathbf{c}^{\mathrm{b}}_{\mathrm{P}}\, \mathbf{t}^{\mathrm{bT}}_{\mathrm{Pk}}\, dm = \int_{Vb} \left\{ \begin{matrix} c_1 \\ c_2 \\ c_3 \end{matrix} \right\}^{\mathrm{b}}_{\mathrm{P}} \left\{ t_1 \; t_2 \; t_3 \right\}^{\mathrm{b}}_{\mathrm{Pk}} dm \tag{vi}$$

Equation (vi) contains all the terms necessary to build equation (i). If finite elements are used to compute (vi), one may proceed in the following manner. First, substitute in (vi) the results of (iv) and (v):

$$\int_{Vb} \mathbf{c}_{\mathrm{P}}^{\mathrm{b}}\, \mathbf{t}_{\mathrm{Pk}}^{\mathrm{bT}}\, dm \;=\; \left[\overline{\mathbf{X}}^{\mathrm{b}}\right]^{-1} \int_{Vb} (\overline{\mathbf{r}}_{\mathrm{P}} - \overline{\mathbf{r}}_{\mathrm{i}})\, \boldsymbol{\phi}_{\mathrm{Pk}}^{\mathrm{bT}}\, dm \;\left[\overline{\mathbf{X}}^{\mathrm{b}}\right]^{-\mathrm{T}} \tag{vii}$$

Now, interpolate the spatial variables (geometry as well as deformed shapes) appearing in the integrand of (vii) using the finite element deformed shapes

$$(\overline{\mathbf{r}}_{\mathrm{P}} - \overline{\mathbf{r}}_{\mathrm{i}}) = \mathbf{N}^{\mathrm{b}}(\overline{\mathbf{r}}_{\mathrm{P}} - \overline{\mathbf{r}}_{\mathrm{i}})\, \overline{\mathbf{x}}^{\mathrm{b}} \tag{viii}$$

$$\boldsymbol{\phi}_{\mathrm{Pk}}^{\mathrm{b}} = \mathbf{N}^{\mathrm{b}}(\overline{\mathbf{r}}_{\mathrm{P}} - \overline{\mathbf{r}}_{\mathrm{i}})\; \mathbf{p}_{\mathrm{k}}^{\mathrm{b}} \tag{ix}$$

where $\mathbf{N}^{\mathrm{b}}(\overline{\mathbf{r}}_{\mathrm{P}} - \overline{\mathbf{r}}_{\mathrm{i}})$ are the finite element functions that are used to interpolate both the geometry as well as the global deformed shapes of the body. The vector $\overline{\mathbf{x}}^{\mathrm{b}}$ represents the coordinates of the finite element mesh, and $\mathbf{p}_{\mathrm{k}}^{\mathrm{b}}$ are the values of k mode in the nodes of the finite element mesh. Substituting the equations (viii) and (ix) in the integral (vii), one can obtain

$$\int_{Vb} \mathbf{c}_{\mathrm{P}}^{\mathrm{b}}\, \mathbf{t}_{\mathrm{Pk}}^{\mathrm{bT}}\, dm \;=\left[\overline{\mathbf{X}}^{\mathrm{b}}\right]^{-1} \int_{Vb} \mathbf{N}^{\mathrm{b}}(\overline{\mathbf{r}}_{\mathrm{P}})\; (\mathbf{x}^{\mathrm{b}}\, \mathbf{p}_{\mathrm{k}}^{\mathrm{bT}}) \left[\mathbf{N}^{\mathrm{b}}(\overline{\mathbf{r}}_{\mathrm{P}})\right]^{\mathrm{T}} dm \;\left[\overline{\mathbf{X}}^{\mathrm{b}}\right]^{-\mathrm{T}} \tag{x}$$

Only interpolation functions are part of the integrand, since the expression inside the parenthesis in the middle of the integral does not depend on the spatial coordinates. The integral (x) may be calculated in a body-by-body basis.

The final step is to express the kinetic energy of the whole multibody system as an addition of the energies of each individual body:

$$T = \sum_{b} T_{\mathrm{b}} = \frac{1}{2}\, \dot{\mathbf{q}}^{\mathrm{T}}\, \mathbf{M}\, \dot{\mathbf{q}} \tag{11.21}$$

where $\mathbf{M}$ and $\dot{\mathbf{q}}$ have been obtained by assembling the submatrices $\mathbf{M}^{\mathrm{b}}$, and vectors $\dot{\mathbf{q}}^{\mathrm{b}}$ and $\dot{\boldsymbol{\eta}}^{\mathrm{b}}$, respectively.

11.2.3 Derivation of the Elastic Potential Energy

The expression for the elastic potential energy takes a very simple form with the moving frame approach, since it is only due to the contribution of the elastic displacement. The overall rigid body motion does not contribute to the potential energy. Consequently, the potential energy of a body is given by

$$\Pi_{\mathrm{b}} = \frac{1}{2}\, \boldsymbol{\eta}^{\mathrm{bT}}\, \mathbf{K}_{\mathrm{ff}}^{\mathrm{b}}\, \boldsymbol{\eta}^{\mathrm{b}} \tag{11.22}$$

where $\mathbf{K}_{\mathrm{s}}^{\mathrm{b}} = \mathbf{K}_{\mathrm{ff}}^{\mathrm{b}}$, if the stiffness has been obtained by using finite elements or

$$\mathbf{K}_{\mathrm{ff}}^{\mathrm{b}} = \overline{\boldsymbol{\Phi}}^{\mathrm{bT}}\, \overline{\mathbf{K}}_{\mathrm{s}}^{\mathrm{b}}\, \overline{\boldsymbol{\Phi}}^{\mathrm{b}} \tag{11.23}$$

by using assumed modes defined in the local frame.

The elastic potential energy of the multibody system is obtained by assembling the potential energies of each of its bodies as:

$$\Pi = \sum_b \Pi_b = \frac{1}{2} \sum_b \left\{ \mathbf{q}^{bT} \; \boldsymbol{\eta}^{bT} \right\} \begin{bmatrix} 0 & 0 \\ 0 & \mathbf{K}_{ff}^b \end{bmatrix} \begin{Bmatrix} \mathbf{q}^b \\ \boldsymbol{\eta}^b \end{Bmatrix} = \frac{1}{2} \mathbf{q}^T \mathbf{K} \mathbf{q} \tag{11.24}$$

where $\mathbf{K}$ is the resulting global stiffness matrix that only affects the subset of $\mathbf{q}$ that corresponds to the elastic displacements $\boldsymbol{\eta}$.

11.2.4 Potential of External Forces

Only the case of a concentrated external force $\mathbf{f}$ that is applied at a point P of the body *b* will be considered in this section. Assuming that the force $\mathbf{f}_p$ is defined in global coordinates and making use of the equation (11.9), the virtual work of this force may be written as:

$$\begin{gathered} \delta W = \delta \mathbf{r}_P^T \mathbf{f}_P = (\delta \mathbf{q}^{bT} \mathbf{C}_P^{bT} + \delta \boldsymbol{\eta}^{bT} \overline{\boldsymbol{\Phi}}_P^{bT} \mathbf{A}^{bT}) \mathbf{f}_P = \\ \left\{ \delta \mathbf{q}^{bT} \; \delta \boldsymbol{\eta}^{bT} \right\} \begin{bmatrix} \mathbf{C}_P^{bT} \\ \overline{\boldsymbol{\Phi}}_P^{bT} \mathbf{A}^{bT} \end{bmatrix} \mathbf{f}_P \end{gathered} \tag{11.25}$$

from which one may find the generalized force

$$\mathbf{Q}_P^b = \begin{bmatrix} \mathbf{C}_P^{bT} \\ \overline{\boldsymbol{\Phi}}_P^{bT} \mathbf{A}^{bT} \end{bmatrix} \mathbf{f}_P \tag{11.26}$$

Consequently, the potential may be easily calculated as

$$V = \int_{qo}^{q} d\mathbf{q}^{bT} \mathbf{Q}_P^b \tag{11.27}$$

The same procedure is used to calculate the generalized force and potential of any other type of loading.

11.2.5 Constraint Equations

The constraint equations for flexible bodies modeled with natural coordinates also come from two different sources, namely, rigid body constraints and joint constraints. The rigid body constraints now correspond to the definition of the moving frame and are derived and formulated as described in Chapter 2. However, the joint constraints must be modified, since these joints also include elastic deformations. As a consequence, variables such as points and unit vectors can no longer be shared at the joints.

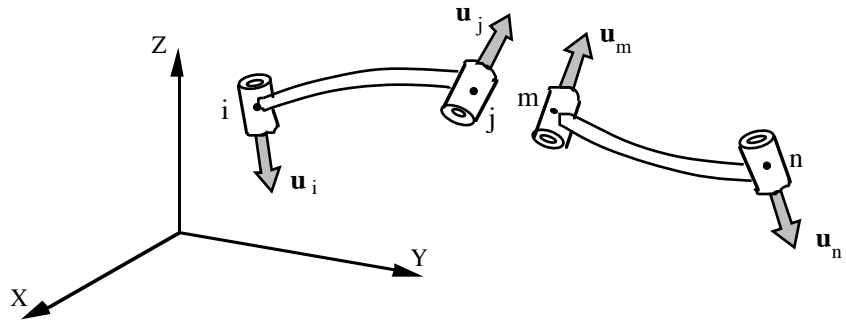

Figure 11.3. Revolute joint between two flexible bodies.

The reason why the variables cannot be shared at the joints is explained with a simple example. Consider the two contiguous bodies *ij* and *mn* shown in figure 11.3, with each of them defined by two points and two vectors. Consider for the moment that the flexibility is modeled by taking for each of them the first cantilever mode. In addition, assume that there is a revolute joint between the two bodies. Now consider that instead of taking two points *j* and *m*, only one point, say *i* , that is shared between the two bodies is taken. Further consider that there is only one vector in the joint, say $\mathbf{u}_j$, which is shared. Note that in the flexible case the natural coordinates do not necessarily coincide with material points or directions, but they are only a mathematical tool to describe the overall motion. Since a joint constraint must be imposed between material points and directions, the sharing of variables does not in this case enforce the revolute joint constraint. Rather, the condition that the deformed end of the body *ij* is coincident with the deformed origin of the body *mn* must be imposed. Since *mn* is clamped at the origin, the previous condition means that the body *ij* cannot deform. This obviously is unacceptable. This reasoning can be extended to more than one mode, but the conclusion is always that the sharing of variables limits the deformation modes in an unacceptable way.

After this consideration, one can now formulate the constraint equations for the revolute joint shown in Figure 11.3. First, the deformed positions of *j* and *m* must coincide. Similarly, the deformed unit vectors $\mathbf{u}_j$ and $\mathbf{u}_m$ must also coincide. Those conditions can be written as:

$$\left(\mathbf{r}_j + \delta\,\mathbf{r}_j\right) - \left(\mathbf{r}_m + \delta\,\mathbf{r}_m\right) = 0 \tag{11.28}$$

$$\left(\mathbf{u}_j + \delta\,\mathbf{u}_j\right) - \left(\mathbf{u}_m + \delta\,\mathbf{u}_m\right) = 0 \tag{11.29}$$

Using expressions (11.5) and (11.6), the displacements $\delta\mathbf{r}_j$, $\delta\mathbf{r}_m$, $\delta\mathbf{u}_j$, and $\delta\mathbf{u}_m$ can be expressed as a linear combination of the Ritz vectors as:

$$\delta \mathbf{r}_j = \mathbf{A}^b \, \delta \bar{\mathbf{r}}_j = \sum_{k=1}^{NR} \eta_k^b(t) \, \mathbf{A}^b \, \bar{\boldsymbol{\phi}}_{jk}^b = \mathbf{A}^b \, \bar{\boldsymbol{\Phi}}_j^b \, \boldsymbol{\eta}^b \tag{11.30}$$

$$\delta \mathbf{u}_j = \mathbf{A}^b \, \delta \bar{\mathbf{u}}_P = \sum_{k=1}^{NR} \eta_k^b(t) \, \mathbf{A}^b \, \bar{\boldsymbol{\phi}}'^b_{Pk} = \mathbf{A}^b \, \bar{\boldsymbol{\Phi}}'^b_P \, \boldsymbol{\eta}^b \tag{11.31}$$

and analogously $\delta\mathbf{r}_m$ and $\delta\mathbf{u}_m$.

The constraint equations for the whole multibody system that can include the definition of relative coordinates at the joints are obtained by putting together all the rigid body and joint constraints in the form

$$\boldsymbol{\Phi}(\mathbf{q}, t) = 0 \tag{11.32}$$

11.2.6 Governing Equations of Motion

Several methods for deriving the equations of motion have been presented in Chapter 4 for rigid body dynamics. The equations of motion in the flexible case are derived in an analogous way, and, therefore, the final form is identical. Having developed expressions for the potential and kinetic energies, the most reasonable way of obtaining the equations of motion is through the Lagrange's equations, which leads to the following result:

$$\mathbf{M}\,\ddot{\mathbf{q}} + \mathbf{K}\,\mathbf{q} + \boldsymbol{\Phi}_\mathbf{q}^T \boldsymbol{\lambda} = \mathbf{Q}_{ex} - \dot{\mathbf{M}}\,\dot{\mathbf{q}} + T_\mathbf{q} \tag{11.33}$$

The last two terms on the RHS of this equation are velocity-dependent in both the rigid and the elastic coordinates. If the second derivative of the constraints is appended, the final form of the equations is

$$\begin{bmatrix} \mathbf{M} & \boldsymbol{\Phi}_\mathbf{q}^T \\ \boldsymbol{\Phi}_\mathbf{q} & 0 \end{bmatrix} \begin{Bmatrix} \ddot{\mathbf{q}} \\ \boldsymbol{\lambda} \end{Bmatrix} = \begin{Bmatrix} \mathbf{Q}_{ex} - \dot{\mathbf{M}}\,\dot{\mathbf{q}} + T_\mathbf{q} - \mathbf{K}\,\mathbf{q} \\ -\dot{\boldsymbol{\Phi}}_\mathbf{q}\,\dot{\mathbf{q}} - \dot{\boldsymbol{\Phi}}_t \end{Bmatrix} \tag{11.34}$$

However, the Lagrange multiplier approach is generally not the best way of integrating these equations of motion. This is due mainly to two reasons: First, the number of constraints and therefore Lagrange multipliers is now much larger than in the rigid body case, since there is not sharing of variables at the joints. Secondly, the elastic terms in the RHS of (11.22) induce a considerable amount of numerical stiffness to the integration process, particularly if high frequency modes of vibrations such as axial modes are present in the formulation.

The first problem can be remedied by the use of the penalty formulation as done in Bayo and Serna (1989) which eliminates the multipliers from the equations of motion; thus reducing considerably the size of the system of equations. Other approaches, described in Chapters 5 and 8 to formulate the equations of motion in independent coordinates using the projection matrix $\mathbf{R}$, can also be applied for flexible multibody dynamics.

Figure 11.4. Flexible space robot in reorientation maneuver.

It is easy to verify that using the penalty formulation, the equations of motion become:

$$\begin{aligned}(\mathbf{M} + \boldsymbol{\Phi}_{\mathbf{q}}^{\mathrm{T}}\boldsymbol{\alpha}\boldsymbol{\Phi}_{\mathbf{q}})\ \ddot{\mathbf{q}} + \mathbf{K}\mathbf{q} = \\ = \mathbf{Q}_{\mathrm{ex}} - \dot{\mathbf{M}}\dot{\mathbf{q}} + T_{\mathbf{q}} - \boldsymbol{\Phi}_{\mathbf{q}}^{\mathrm{T}}\boldsymbol{\alpha}\,(\dot{\boldsymbol{\Phi}}_{\mathbf{q}}\dot{\mathbf{q}} + 2\boldsymbol{\mu}\boldsymbol{\Omega}\,\dot{\boldsymbol{\Phi}} + \boldsymbol{\Omega}^{2}\boldsymbol{\Phi})\end{aligned} \tag{11.35}$$

The second problem, which is related to the stiffness of the resulting equations, may be solved by using the *A*-stable numerical algorithms presented in Chapter 7. The most appropriate implementation of these algorithms for the case at hand is that explained in Chapter 8, Section 8.5. In this explanation, the difference equations of the integrator are substituted into the equations of motion. The resulting set of nonlinear equations is solved using Newton-Raphson iteration.

11.2.7 Numerical Example

Using the method presented above, a satellite deployment maneuver has been simulated, where a flexible robot turns and repositions a satellite. Figure 11.4 shows the complete system, and Figure 11.5 shows the set of points and vectors used to define the mathematical model. The main links of the robot (bodies 3 and 4) are assumed to be flexible and have been modeled using six beam elements, while the other links of the robot (end-effector, wrist) are assumed rigid. The main body of the satellite is supposed rigid, while the solar arrays are flexible and modeled with eleven beam elements of equivalent stiffness and mass. An inertial reference frame is located at the base of the manipulator on the shuttle bay.

Figure 11.5. Natural coordinates model of a flexible robot.

Figure 11.6. Deviation of the x-coordinate of the robot end-effector.

The input to the system is a known variation of the angles driving the manipulator that leads to the desired motion of the system. This motion is a 90 degrees rotation around the Z axis, and, simultaneously, a 180 degrees rotation around the Y axis, in order to re-orientate the satellite. Using this input, the dynamic response of the system has been calculated. Figure 11.6 shows the deviation of the position of the robot end-effector (x-coordinate) relative to the rigid body motion that represents the elastic vibration response superimposed on the large rigid body motion. Once the driving input is finished at time 600 sec., a residual vibration remains in the system due to the absence of damping. Calculations have been carried out on a Silicon Graphics Power Iris 4D/240 computer, using only one processor. The required CPU time has been about 2000 sec. for a maneuver that lasts 800 sec. in real time.

11.3 Global Method Based on Large Rotation Theory

The methods in this section are contributions from Avello (1990).

As mentioned in the overview of the different methods, the classical moving frame approach is based on the assumption of small displacements and equilibrium in the undeformed configuration. Kane, Ryan, and Banerjee (1987) showed that these assumptions lead to a spurious loss of stiffness, when the rotational velocities are large. Moreover, the method seen in the previous section cannot handle larger displacements than those for which the linear finite element method yields accurate results.

When both the elastic displacements are small and the stiffening effects are not important, the classical method yields sufficiently accurate results. It is usually preferred because of the reduced number of equations and the possibility of using either assumed or experimentally found modes of vibration. When the stiffening effects become important and/or displacements become finite, the global or absolute method described in this section can be applied. It is called global or absolute because the entire motion of the body (finite rotation plus deformation) is all referred to a fixed frame. This produces a shifting of non-linearity from the inertia terms in the moving frame approach to the deformation terms in this new approach. A formulation of this type was first presented by Simo and Vu-Quoc (1986 and 1988) for multibodies modeled as planar and three-dimensional beams, respectively.

In this section it will be assumed that the flexible bodies are long and slender and that they can be correctly modeled as beams. Timoshenko's beam theory will be used, under the basic assumption that plane sections initially normal to the centroidal line remain plane after global deformation has taken place. With these basic assumption, one will derive expressions for a simple nonlinear finite element method that can be used to model flexible bodies in a multibody formalism. The most attractive features of this formulation are its simplicity and the compatibility with the natural coordinates so far used in this book, since the nodal variables of the new beam element are also Cartesian points and unit vectors.

11.3.1 Kinematics of the Beam

Figure 11.7 shows an initially straight prismatic beam of length L and constant cross section A. One can define a fixed reference frame (X_1, X_2, X_3), with the X_1 axis coincident with the centroidal line, and axes X_2 and X_3 coincident with the principal axes of inertia. Any cross section of the beam can be described in this initial state by the coordinates (X_1, 0, 0) of the intersection point between the cross section and the centroidal line, and by two mutually orthogonal vectors **M** and **N** parallel to the X_2 and X_3 axes. Vectors **M** and **N** can be considered as *co-rotational vectors* that move rigidly attached to the cross section to which they belong.

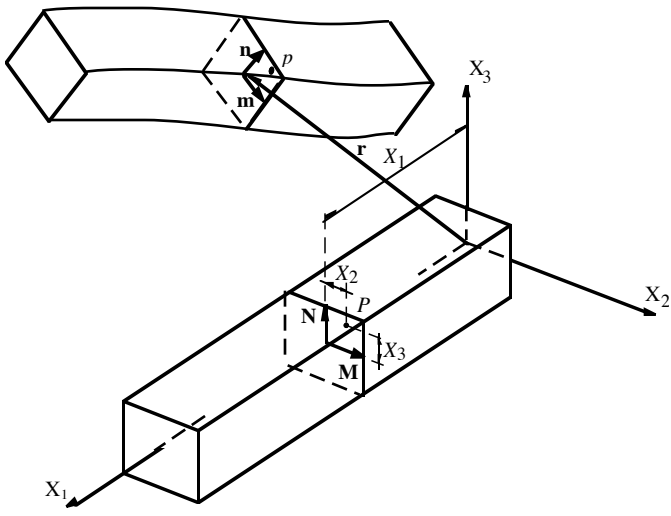

Figure 11.7. Deformed and undeformed prismatic 3-D beam.

After the beam has undergone finite displacements, the position of its cross sections can be defined with the coordinates of the intersection point **r** and with the components of the co-rotational vectors **m** and **n**, as shown in Figure 11.7. Upper-case letters will be used for the undeformed positions (*material coordinates*) and lower-case letters for deformed positions (*spatial coordinates*). If a Lagrangian formulation is used, one can write the deformed positions as a function of the undeformed ones. Since the initially straight prismatic beam is characterized in its undeformed position by just the X_1 coordinate, vectors **r**, **m**, and **n** can be written as a function of X_1, and the time t, as $\mathbf{r}=\mathbf{r}(X_1, t)$, $\mathbf{m}=\mathbf{m}(X_1, t)$, and $\mathbf{n}=\mathbf{n}(X_1, t)$. The deformed coordinates $\mathbf{x}=(x_1, x_2, x_3)$ of a particle whose material coordinates are $\mathbf{X}=(X_1, X_2, X_3)$ can be written as

$$\mathbf{x}(\mathbf{X}, t) = \mathbf{r}(X_1, t) + X_2\,\mathbf{m}(X_1, t) + X_3\,\mathbf{n}(X_1, t) \tag{11.36}$$

where X_1 is not a function of time.

11.3.2 A Nonlinear Beam Finite Element Formulation

In the finite element method, a proper inter-element continuity for the interpolated function and its derivatives must be assured by the shape functions. Typical Timoshenko beam elements require continuity only in the displacements and rotations but not in their derivatives (C^0 continuity). This is achieved by interpolating independently the displacements and rotations inside each element. In this section, an independent interpolation will be assumed for the nodal variables. However, the nodal variables that will be used in this section are different, in na-

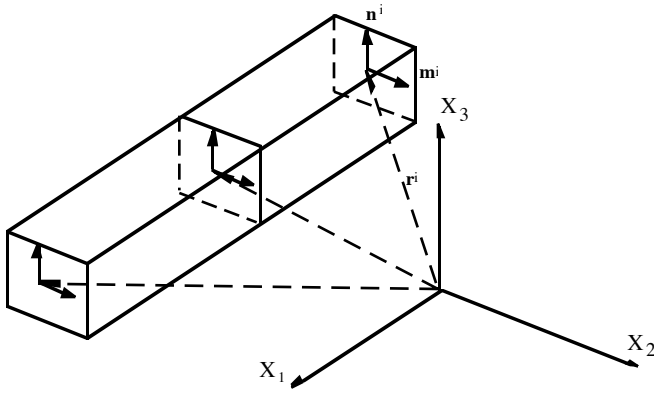

Figure 11.8. Cartesian dependent coordinates for a beam section.

ture and number, from the classical nodal variables used in linear beam elements. The nodal variables in the classical beam elements are composed of three displacements u_i and three rotations θ_i. Instead, the *nodal variables* used here are composed of the three coordinates of the position $\mathbf{r}^i$ and the six components of the two orthogonal unit vectors $\mathbf{m}^i$ and $\mathbf{n}^i$, as shown in Figure 11.8.

The nine nodal variables ($\mathbf{r}^i$, $\mathbf{m}^i$, $\mathbf{n}^i$) are redundant, because only three of the six components of $\mathbf{m}^i$ and $\mathbf{n}^i$ are independent. In fact, there are three constraint equations that $\mathbf{m}^i$ and $\mathbf{n}^i$ must satisfy, two corresponding to the unit norm condition and the third corresponding to the orthogonality condition between them. Redundant variables have been extensively used in the kinematic and dynamic analysis of multibody systems, as has been seen throughout this book, but seldom in the finite element method. The main advantage of using redundant variables is that the overall complexity of the formulation is reduced. The degree of non-linearity of the problem is reduced as the number of variables is increased. The cost that one has to pay is the introduction of constraint equations to enforce the satisfaction of the constraints at the nodes.

Let ($\mathbf{r}^i$, $\mathbf{m}^i$, $\mathbf{n}^i$), $i = 1, \ldots, p^e$ be the values of ($\mathbf{r}$, $\mathbf{m}$, $\mathbf{n}$) in the p^e nodes that belong to the finite element e. The values of ($\mathbf{r}$, $\mathbf{m}$, $\mathbf{n}$) inside each finite element are obtained through the following interpolation scheme:

$$\mathbf{r}^e = \sum_{i=1}^{p^e} N_i \mathbf{r}^i, \qquad \mathbf{m}^e = \sum_{i=1}^{p^e} N_i \mathbf{m}^i, \qquad \mathbf{n}^e = \sum_{i=1}^{p^e} N_i \mathbf{n}^i \tag{11.37}$$

where N_i are the shape functions that can be found in any standard book in the finite element method (See Bathe (1982)).

Note that in expression (11.37) unit vectors are being interpolated. Since the shape functions are not required to preserve the norm, vectors $\mathbf{m}^e$ and $\mathbf{n}^e$ have no longer a unit module. In the same way, the interpolated values $\mathbf{m}^e$ and $\mathbf{n}^e$ are not orthogonal. This interpolation inconsistency adds a new source of numerical er-

ror that is added to the global error of the finite element method. A full discussion on how this error affects the accuracy of the solution goes beyond the scope of this chapter, but the following points may give more insight.

– First, the magnitude of the interpolation errors depends on the relative rotation among the nodes of a single finite element. This means that small relative rotations imply small interpolation errors. For example, one can interpolate the two vectors:

$$\mathbf{m}^1 = \begin{Bmatrix} 0 \\ 1 \end{Bmatrix} \qquad \mathbf{m}^2 = \begin{Bmatrix} cos\ \varphi \\ sin\ \varphi \end{Bmatrix} \tag{11.38}$$

with the linear shape functions:

$$N_1 = \frac{L - x}{L} \qquad N_1 = \frac{x}{L} \tag{11.39}$$

The resulting interpolated vector inside the element can be obtained as

$$\mathbf{m}^{\mathrm{e}} = N_1 \mathbf{m}^1 + N_2 \mathbf{m}^2 \tag{11.40}$$

The module of this vector can be easily calculated as:

$$\mathbf{m}^{\mathrm{eT}} \mathbf{m}^{\mathrm{e}} = N_1^2 + N_2^2 + 2 N_1 N_2 \mathbf{m}^{1\mathbf{T}} \mathbf{m}^2 = 2 \left(\frac{x^2}{L^2} - \frac{x}{L} \right) \left(1 - cos\ \varphi \right) + 1 \tag{11.41}$$

The maximum constraint violation is obtained in the middle of the element. Take φ=10 degrees and compute the module of $\mathbf{m}^{\mathbf{e}}$ by taking the square root of equation (11.41). The resulting value is $|\mathbf{m}^{\mathbf{e}}|$=0.996195, which represents an error below the 0.4%. Since one does not expect to handle rotations larger than 10 degrees among the nodes of the same finite element, the approximation seems quite reasonable.

– Secondly, the convergence of the finite element method is guaranteed, because as the number of elements increases the error due to the interpolation decreases. In the limit, no error is obtained.
– Finally, the results obtained with this formulation are similar to the ones obtained with other nonlinear formulations.

11.3.3 Derivation of the Kinetic Energy

In order to obtain the inertia forces, one must first develop the expression for the kinetic energy, which can be obtained from the integral:

$$T^{\mathrm{e}} = \frac{1}{2} \int_{V^e} \dot{\mathbf{x}}^{\mathrm{eT}} \dot{\mathbf{x}}^{\mathrm{e}}\, dm \tag{11.42}$$

The velocity of a material point $\dot{\mathbf{x}}^e$ is obtained by differentiating expression (11.36) particularized for element *e*, and by substituting the interpolation scheme given in (11.37). This leads to

$$\dot{\mathbf{x}}^{\mathrm{e}} = \sum_{i=1}^{p^e} N_{\mathrm{i}} \left(\dot{\mathbf{r}}^{\mathrm{i}} + X_2 \, \dot{\mathbf{m}}^{\mathrm{i}} + X_3 \, \dot{\mathbf{n}}^{\mathrm{i}} \right) \tag{11.43}$$

Substituting equation (11.43) into (11.42) yields

$$T^{\mathrm{e}} = \frac{1}{2} \int_{V^e} \sum_{i=1}^{p^e} \sum_{j=1}^{p^e} N_{\mathrm{i}} \, N_{\mathrm{j}} \left(\dot{\mathbf{r}}^{\mathrm{iT}} \, \dot{\mathbf{r}}^{\mathrm{j}} + X_2^2 \, \dot{\mathbf{m}}^{\mathrm{iT}} \, \dot{\mathbf{m}}^{\mathrm{j}} + X_3^2 \, \dot{\mathbf{n}}^{\mathrm{iT}} \, \dot{\mathbf{n}}^{\mathrm{j}} + \right.$$

$$\left. + 2 \, X_2 \, \dot{\mathbf{r}}^{\mathrm{iT}} \, \dot{\mathbf{m}}^{\mathrm{j}} + 2 \, X_3 \, \dot{\mathbf{r}}^{\mathrm{iT}} \, \dot{\mathbf{n}}^{\mathrm{j}} + X_2 \, X_3 \, \dot{\mathbf{m}}^{\mathrm{iT}} \, \dot{\mathbf{n}}^{\mathrm{j}} \right) dm \tag{11.44}$$

where the only terms that depend on the variables of the integral are X_2 and X_3. Since X_2 and X_3 are principal axes of inertia and recalling that X_1 coincides with the center of gravity of the cross section, the three last terms in the integral vanish, because they represent two static moments of first order and an inertia product. After reordering equation (11.44), the standard form of the kinetic energy is obtained as

$$T^{\mathrm{e}} = \frac{1}{2} \, \dot{\mathbf{q}}^{\mathrm{eT}} \, \mathbf{M}^{\mathrm{e}} \, \dot{\mathbf{q}}^{\mathrm{e}} \tag{11.45}$$

where $\mathbf{q}^{\mathrm{e}}$ is a vector that contains the nodal variables of element e as

$$\mathbf{q}^{\mathrm{eT}} = \left\{ \mathbf{r}^{1\mathrm{T}} \, \mathbf{m}^{1\mathrm{T}} \, \mathbf{n}^{1\mathrm{T}} \; \cdots \; (\mathbf{r}^{\mathrm{p^e}})^{\mathrm{T}} \, (\mathbf{m}^{\mathrm{p^e}})^{\mathrm{T}} \, (\mathbf{n}^{\mathrm{p^e}})^{\mathrm{T}} \right\} \tag{11.46}$$

The matrix $\mathbf{M}^{\mathrm{e}}$ is constant, symmetric, and is composed of sparse submatrices $\mathbf{M}_{\mathrm{ij}}$ of size (9x9). In an homogeneous beam, $\mathbf{M}^{\mathrm{e}}$ takes the form:

$$\mathbf{M}^{\mathrm{e}} = \begin{bmatrix} \mathbf{M}_{11} & \mathbf{M}_{12} & \cdots & \mathbf{M}_{1p^e} \\ \mathbf{M}_{21} & \mathbf{M}_{22} & \cdots & \mathbf{M}_{2p^e} \\ \cdots & \cdots & \cdots & \cdots \\ \mathbf{M}_{p^e1} & \mathbf{M}_{p^e2} & \cdots & \mathbf{M}_{p^ep^e} \end{bmatrix} \tag{11.47}$$

$$\mathbf{M}_{\mathrm{ij}} = \rho \begin{bmatrix} A \, c_{\mathrm{ij}} \, \mathbf{I}_3 & \mathbf{0}_3 & \mathbf{0}_3 \\ \mathbf{0}_3 & I_2 \, c_{\mathrm{ij}} \, \mathbf{I}_3 & \mathbf{0}_3 \\ \mathbf{0}_3 & \mathbf{0}_3 & I_3 \, c_{\mathrm{ij}} \, \mathbf{I}_3 \end{bmatrix} \tag{11.48}$$

where ρ is the volumetric density, $\mathbf{I}_3$ the (3×3) unit matrix, and c_{ij} the integral over the length of the element of the product of shape functions ($N_i \, N_j$).

Compare this simple and constant expression for the mass matrix with the highly nonlinear matrix obtained in Section 11.2.3. Although the mass matrix is simpler, the elastic potential energy in the next section is more complicated than with the moving frame method.

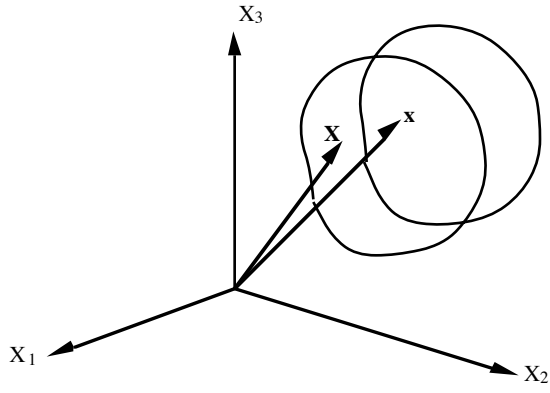

Figure 11.9. Undeformed and deformed position vectors of a point.

11.3.4 Derivation of the Elastic Potential Energy

One of the basic assumptions often made in structural theory is that displacements and displacement gradients are small. When this assumption holds, the *Cauchy strain tensor* can be used and accurate results are given. However, the Cauchy strain tensor does not work for large displacements, since it does not exhibit the proper invariance under rigid body rotations of the displacement field. Therefore, when large rotations are considered, a different measure of the strain must be used.

Several different kinds of strain measures have been proposed when displacements, displacement gradients, or both are finite (Malvern (1969)). These strain measures can be included in two major groups. *Eulerian formulations* formulate the problem in the deformed configuration, while *Lagrangian formulations* formulate it in the undeformed configuration. Eulerian formulations are used in applications where an undeformed or initial state does not exist or is unknown, as in fluid mechanics. In elasticity, however, it seems more useful to use a Lagrangian formulation, since an undeformed configuration is always assumed to exist and is taken as a reference state.

The *Green strain tensor* has typically been used in nonlinear elasticity to characterize the deformation field of bodies undergoing large displacements. As the displacements and displacement gradients get smaller, the Green tensor tends to the Cauchy tensor and, in the limit, they are identical.

Consider a continuous body and a fixed reference frame (X_1, X_2, X_3), as can be seen in Figure 11.9. Capital letters $\mathbf{X}=(X_1, X_2, X_3)$ will be used to refer to the coordinates of a particle in an initially undeformed position, and lower-case letters $\mathbf{x}=(x_1, x_2, x_3)$ will be used for the currently deformed position. In a Lagrangian formulation, $\mathbf{x}$ is taken as a function of $\mathbf{X}$ and time, and therefore can be written

$$\mathbf{x} = \mathbf{x}(\mathbf{X}, t) \tag{11.49}$$

The *deformation gradient* $\mathbf{F}$ is defined as the matrix that contains the partial derivatives of $\mathbf{x}$ with respect to $\mathbf{X}$. An infinitesimal vector in the deformed position $d\mathbf{x}$ can be expressed in terms of the deformation gradient and of its undeformed position $d\mathbf{X}$ as

$$d\mathbf{x} = \frac{\partial \mathbf{x}}{\partial \mathbf{X}} d\mathbf{X} = \mathbf{F}\, d\mathbf{X} \tag{11.50}$$

The *Green deformation tensor* $\mathbf{C}$ is defined as the one that gives the new squared length $(ds)^2$ of vector $d\mathbf{x}$, into which the given vector $d\mathbf{X}$ has deformed. Thus,

$$ds^2 = d\mathbf{X}^{\mathrm{T}}\, \mathbf{C}\, d\mathbf{X} \tag{11.51}$$

The *Green strain tensor* $\mathbf{E}$ gives, by definition, the change in squared length between the deformed and the undeformed state of a vector $d\mathbf{X}$

$$ds^2 - dS^2 = 2\, d\mathbf{X}^{\mathrm{T}}\, \mathbf{E}\, d\mathbf{X} \tag{11.52}$$

where $(dS)^2$ is the original length of vector $d\mathbf{X}$. Comparing equations (11.50), (11.51), and (11.52), the two following relations can easily be found:

$$\mathbf{C} = \mathbf{F}^{\mathrm{T}}\, \mathbf{F} \tag{11.53}$$

$$\mathbf{E} = \frac{\mathbf{C} - \mathbf{I}_3}{2} \tag{11.54}$$

where $\mathbf{I}_3$ is the (3×3) identity matrix.

The potential energy for a linearly elastic homogeneous material can be written in terms of the strain vector $\mathbf{E} = \{E_{11}\, E_{22}\, E_{33}\, E_{12}\, E_{13}\, E_{23}\}^{\mathrm{T}}$ as

$$V = \frac{1}{2} \int_{V^e} \mathbf{E}^{\mathrm{T}}\, \mathbf{D}\, \mathbf{E}\, dV \tag{11.55}$$

where the integral is extended to the body in the undeformed configuration. $\mathbf{D}$ represents the matrix of elastic constants, which is defined in terms of *Lame's* constants λ and G as

$$\mathbf{D} = \begin{bmatrix} \lambda + 2G & \lambda & \lambda & 0 & 0 & 0 \\ \lambda & \lambda + 2G & \lambda & 0 & 0 & 0 \\ \lambda & \lambda & \lambda + 2G & 0 & 0 & 0 \\ 0 & 0 & 0 & 2G & 0 & 0 \\ 0 & 0 & 0 & 0 & 2G & 0 \\ 0 & 0 & 0 & 0 & 0 & 2G \end{bmatrix} \tag{11.56}$$

The values of λ and G in terms of the *Young modulus* E and the *Poisson ratio* ν are:

$$\lambda = \frac{E\,\nu}{(1+\nu)(1-2\,\nu)} \qquad G = \frac{E}{2(1+\nu)} \tag{11.57}$$

As seen in equation (11.36), the deformed coordinates of any point of the beam can be written as

$$\mathbf{x}(\mathbf{X}, t) = \mathbf{r}(X_1, t) + X_2\,\mathbf{m}(X_1, t) + X_3\,\mathbf{n}(X_1, t) \tag{11.58}$$

The deformation gradient $\mathbf{F}$ can be easily computed as

$$\mathbf{F} = \frac{\partial \mathbf{x}}{\partial \mathbf{X}} = [\ \mathbf{x}_{,1} \mid \mathbf{x}_{,2} \mid \mathbf{x}_{,3}\ ] = [\ \mathbf{r}_{,1} + X_2\,\mathbf{m}_{,1} + X_3\,\mathbf{n}_{,1} \mid \mathbf{m} \mid \mathbf{n}\ ] \tag{11.59}$$

where the vertical bars in equation indicate the separation between columns. The notation $(-)_{,i}$ is used to represent $\partial(-)/\partial X_i$. The Green strain tensor can be obtained by substituting equation (11.59) into equations (11.53) and (11.54) as

$$\mathbf{E} = \frac{1}{2}\begin{bmatrix} \mathbf{x}_{,1}^{\mathrm{T}}\,\mathbf{x}_{,1} - 1 & \mathbf{x}_{,1}^{\mathrm{T}}\,\mathbf{m} & \mathbf{x}_{,1}^{\mathrm{T}}\,\mathbf{n} \\ \mathbf{x}_{,1}^{\mathrm{T}}\,\mathbf{m} & 0 & 0 \\ \mathbf{x}_{,1}^{\mathrm{T}}\,\mathbf{n} & 0 & 0 \end{bmatrix} \tag{11.60}$$

with

$$\mathbf{x}_{,1} = \mathbf{r}_{,1} + X_2\,\mathbf{m}_{,1} + X_3\,\mathbf{n}_{,1} \tag{11.61}$$

Substituting equation (11.61) into (11.60) and operating, the following expression is obtained for the components of the strain vector $\mathbf{E}$:

$$\begin{aligned} E_{11} = \frac{1}{2}\left(\mathbf{x}_{,1}^{\mathrm{T}}\,\mathbf{x}_{,1} - 1\right) = \frac{1}{2}\Big(\mathbf{r}_{,1}^{\mathrm{T}}\,\mathbf{r}_{,1} + X_2^2\,\mathbf{m}_{,1}^{\mathrm{T}}\,\mathbf{m}_{,1} + X_3^2\,\mathbf{n}_{,1}^{\mathrm{T}}\,\mathbf{n}_{,1} + \\ + 2\,X_2\,\mathbf{r}_{,1}^{\mathrm{T}}\,\mathbf{m}_{,1} + 2\,X_3\,\mathbf{r}_{,1}^{\mathrm{T}}\,\mathbf{n}_{,1} + 2\,X_2\,X_3\,\mathbf{m}_{,1}^{\mathrm{T}}\,\mathbf{n}_{,1} - 1\Big) \end{aligned} \tag{11.62a}$$

$$E_{22} = E_{33} = 0 \tag{11.62b}$$

$$E_{12} = \frac{1}{2}\mathbf{x}_{,1}^{\mathrm{T}}\,\mathbf{m} = \frac{1}{2}\left(\mathbf{r}_{,1}^{\mathrm{T}}\,\mathbf{m} + X_2\,\mathbf{m}_{,1}^{\mathrm{T}}\,\mathbf{m} + X_3\,\mathbf{n}_{,1}^{\mathrm{T}}\,\mathbf{m}\right) \tag{11.62c}$$

$$E_{13} = \frac{1}{2}\mathbf{x}_{,1}{}^{\mathrm{T}}\,\mathbf{n} = \frac{1}{2}\left(\mathbf{r}_{,1}^{\mathrm{T}}\,\mathbf{n} + X_2\,\mathbf{m}_{,1}^{\mathrm{T}}\,\mathbf{n} + X_3\,\mathbf{n}_{,1}^{\mathrm{T}}\,\mathbf{n}\right) \tag{11.62d}$$

$$E_{23} = 0 \tag{11.62e}$$

If it is assumed that the strains are sufficiently small (note, however, that finite elastic displacements and rotations are still being considered), the products $(\mathbf{m}_{,1}^{\mathrm{T}}\,\mathbf{m}_{,1})$, $(\mathbf{n}_{,1}^{\mathrm{T}}\,\mathbf{n}_{,1})$, and $(\mathbf{m}_{,1}^{\mathrm{T}}\,\mathbf{n}_{,1})$ in E_1 are second-order terms that can be neglected. Furthermore, the products $(\mathbf{m}_{,1}^{\mathrm{T}}\,\mathbf{m})$ and $(\mathbf{n}_{,1}^{\mathrm{T}}\,\mathbf{n})$ are zero, as can easily be seen by differentiating with respect to X_1 the two unit norm conditions $(\mathbf{m}^{\mathrm{T}}\,\mathbf{m} - 1 = 0)$ and $(\mathbf{n}^{\mathrm{T}}\,\mathbf{n} - 1 = 0)$, respectively. With these simplifications, the strain measures can finally be written as:

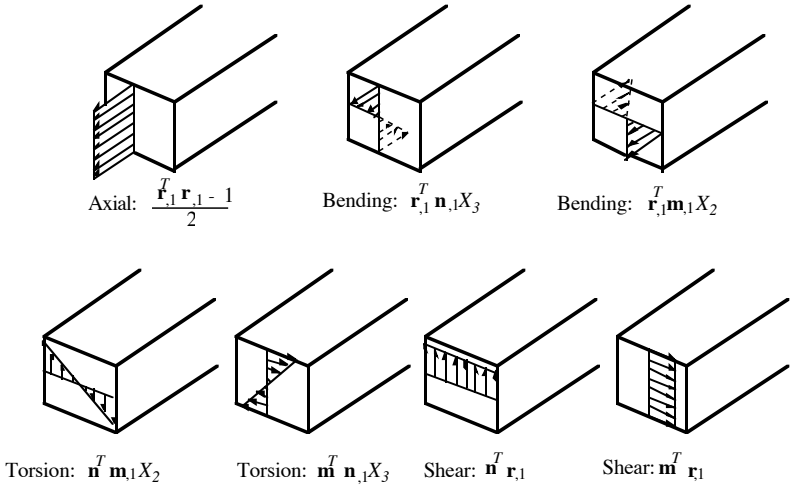

Figure 11.10. Axial, bending, torsion, and shear strains in a beam.

$$E_{11} = \frac{1}{2}\left(\mathbf{r}_{,1}^{\mathrm{T}} \mathbf{r}_{,1} - 1 + 2\, X_2\, \mathbf{r}_{,1}^{\mathrm{T}} \mathbf{m}_{,1} + 2\, X_3\, \mathbf{r}_{,1}^{\mathrm{T}} \mathbf{n}_{,1} \right) \tag{11.63a}$$

$$E_{22} = E_{33} = E_{23} = 0 \tag{11.63b}$$

$$E_{12} = \frac{1}{2}\left(\mathbf{r}_{,1}^{\mathrm{T}} \mathbf{m} + X_3\, \mathbf{n}_{,1}^{\mathrm{T}} \mathbf{m} \right) \tag{11.63c}$$

$$E_{13} = \frac{1}{2}\left(\mathbf{r}_{,1}^{\mathrm{T}} \mathbf{n} + X_2\, \mathbf{m}_{,1}^{\mathrm{T}} \mathbf{n} \right) \tag{11.63d}$$

which is in accordance with the strain distribution predicted by the elemental theory of strength of materials for a prismatic beam under axial, shearing, bending, and torsion loads, as illustrated in Figure 11.10. For example, the term $(\mathbf{r}_{,1}^T \mathbf{r}_{,1} - 1)/2$ in E_{11} represents a constant strain distribution corresponding to a pure axial load. Analogously, the term $(X_2\, \mathbf{r}_{,1}^{\mathrm{T}} \mathbf{m}_{,1})$ in E_{11} represents a strain distribution that varies linearly with X_2, with a zero value at the centroid and extreme values at the edges, as corresponds to a pure bending load. The two constant shear strains predicted by the Timoshenko beam theory are known to be incorrect, and a parabolic strain distribution should appear. This has typically been corrected by multiplying the area of the cross section by a factor (5/6 for rectangular sections) which gives the correct shear strain energy of the beam.

The potential energy of a single element can now be written as

$$\Pi^{\mathrm{e}} = \frac{1}{2} \int_V \left(E\, E_{11}^2 + 2\, G\, E_{12}^2 + 2\, G\, E_{13}^2 \right) dV \tag{11.64}$$

Substituting equation (11.63) and operating, one can obtain

$$\Pi^{\mathrm{e}} = \frac{1}{2}\int_V \Big[E\,A\,\Gamma_1^{\,2} + E\,I_2\,\Gamma_2^{\,2} + E\,I_3\,\Gamma_3^{\,2} + G\,A_{s2}\,\Gamma_4^{\,2} + \\ + G\,A_{s3}\,\Gamma_5^{\,2} + G\,I_p\,\Gamma_6^{\,2}\Big]\,dX_1 \tag{11.65}$$

where Γ_1 represents the axial strain, Γ_2 and Γ_3 are the bending unit rotations per unit length, Γ_4 and Γ_5 are the shearing strains, and Γ_6 is the torsion rotation per unit length. Their expressions are:

$$\Gamma_1 = \frac{\mathbf{r}_{,1}^{\mathrm{T}}\,\mathbf{r}_{,1} - 1}{2} \qquad \Gamma_2 = \mathbf{r}_{,1}^{\mathrm{T}}\,\mathbf{n}_{,1} \qquad \Gamma_3 = \mathbf{r}_{,1}^{\mathrm{T}}\,\mathbf{m}_{,1}$$
$$\Gamma_4 = \mathbf{r}_{,1}^{\mathrm{T}}\,\mathbf{m} \qquad \Gamma_5 = \mathbf{r}_{,1}^{\mathrm{T}}\,\mathbf{n} \qquad \Gamma_6 = \mathbf{n}_{,1}^{\mathrm{T}}\,\mathbf{m} \tag{11.66}$$

where A_{s2} and A_{s3} are the equivalent shear areas, and I_2, I_3, and I_p have the following meaning:

$$I_2 = \int_A X_3^2\,dA \qquad I_3 = \int_A X_2^2\,dA \qquad I_p = \int_A (X_2^2 + X_3^2)\,dA \tag{11.67}$$

The finite element interpolation given in equation (11.37) can be introduced into equations (11.65) and (11.66). After some algebraic manipulations and rearrangements, the following expressions for the strains Γ_i can be obtained:

$$\Gamma_i = \frac{1}{2}\,\mathbf{q}^{\mathrm{eT}}\,\mathbf{G}^{\mathrm{i}}\,\mathbf{q}^{\mathrm{e}} - \beta_i, \qquad i = 1, \cdots, 6 \tag{11.68}$$

with $\beta_1 = 1/2$, $\beta_i = 0$, $i = 2, \ldots, 6$, and where $\mathbf{q}^{\mathrm{e}}$ was defined in (11.46). The matrices $\mathbf{G}^{\mathrm{i}}$ are symmetric, sparse, and depend only on the shape functions and their derivatives with respect to X_1. Their expressions are as follows:

$$\mathbf{G}^1 = \begin{bmatrix} N_{\mathrm{i},1}\,N_{\mathrm{j},1}\,\mathbf{I}_3 & 0_3 & 0_3 \\ 0_3 & 0_3 & 0_3 \\ 0_3 & 0_3 & 0_3 \end{bmatrix} \tag{11.69a}$$

$$\mathbf{G}^2 = \begin{bmatrix} 0_3 & 0_3 & N_{\mathrm{i},1}\,N_{\mathrm{j},1}\,\mathbf{I}_3 \\ 0_3 & 0_3 & 0_3 \\ N_{\mathrm{i},1}\,N_{\mathrm{j},1}\,\mathbf{I}_3 & 0_3 & 0_3 \end{bmatrix} \tag{11.69b}$$

$$\mathbf{G}^3 = \begin{bmatrix} 0_3 & N_{\mathrm{i},1}\,N_{\mathrm{j},1}\,\mathbf{I}_3 & 0_3 \\ N_{\mathrm{i},1}\,N_{\mathrm{j},1}\,\mathbf{I}_3 & 0_3 & 0_3 \\ 0_3 & 0_3 & 0_3 \end{bmatrix} \tag{11.69c}$$

$$\mathbf{G}^4 = \begin{bmatrix} 0_3 & N_{\mathrm{i},1}\,N_{\mathrm{j}}\,\mathbf{I}_3 & 0_3 \\ N_{\mathrm{j},1}\,N_{\mathrm{i}}\,\mathbf{I}_3 & 0_3 & 0_3 \\ 0_3 & 0_3 & 0_3 \end{bmatrix} \tag{11.69d}$$

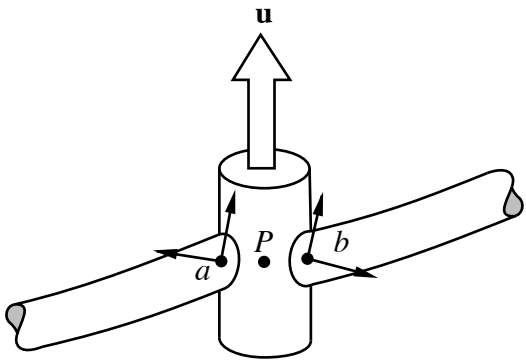

Figure 11.11. Definition of a revolute joint.

$$\mathbf{G}^5 = \begin{bmatrix} 0_3 & 0_3 & N_{\mathrm{i},1}\, N_{\mathrm{j}}\, \mathbf{I}_3 \\ 0_3 & 0_3 & 0_3 \\ N_{\mathrm{j},1}\, N_{\mathrm{i}}\, \mathbf{I}_3 & 0_3 & 0_3 \end{bmatrix} \tag{11.69e}$$

$$\mathbf{G}^6 = \begin{bmatrix} 0_3 & 0_3 & 0_3 \\ 0_3 & 0_3 & N_{\mathrm{j},1}\, N_{\mathrm{i}}\, \mathbf{I}_3 \\ 0_3 & N_{\mathrm{i},1}\, N_{\mathrm{j}}\, \mathbf{I}_3 & 0_3 \end{bmatrix} \tag{11.69f}$$

The total potential energy for the beam is obtained by adding the potential energy of all the elements given by expressions (11.65), (11.68), and (11.69) as

$$\Pi = \sum_{\mathrm{e}} \Pi^{\mathrm{e}} \tag{11.70}$$

Observe that in this beam element the potential energy is obtained as a polynomial of order 4 in the position variables because Π^e depends on the square of Γ_i, and Γ_i depends on the square of $\mathbf{q}^{\mathrm{e}}$. It is unlike the classical moving frame formulation of Section 11.2, in which the potential energy is a quadratic function of the position variables. This complicates the implementation of the elastic forces, but the mass matrix obtained in Section 11.3.3 is constant and can be computed only once. Therefore, the complexity is transferred from the inertia forces to the elastic forces, but the overall complexity remains similar to the moving frame method's complexity.

11.3.5 Constraint Equations

Since the position variables are not independent, constraints must be introduced at the finite element nodes and at the joints. The constraints at the nodes account for the unit norm and orthogonality conditions that the unit vectors must satisfy.

The constraints at the joints restrict the relative motion of adjacent bodies to the rotations or translations allowed by the kinematic joints.

Each node introduces six constraints of the form

$$\begin{Bmatrix} \mathbf{l}_i^T \mathbf{l}_i - 1 \\ \mathbf{l}_i^T \mathbf{m}_i \\ \mathbf{m}_i^T \mathbf{m}_i - 1 \\ \mathbf{m}_i^T \mathbf{n}_i \\ \mathbf{n}_i^T \mathbf{n}_i - 1 \\ \mathbf{n}_i^T \mathbf{l}_i \end{Bmatrix} = 0 \tag{11.71}$$

The constraint equations at the joints can be written in terms of the nodal variables of the nodes next to the joint. The constraint equations for a revolute joint are presented below as an example. Figure 11.11 shows two beam-like bodies linked at point P by a revolute joint of axis $\mathbf{u}$. Let a and b be the two nodes next to the joint, each of them belonging to one of the beams. The revolute joint constraints must enforce both the condition that point P as attached to the frame in a and as attached to the frame in b coincides, and the condition that the vector $\mathbf{u}$ as attached to a and as attached to b also coincide. Both conditions can be written through the following two vector equations equivalent to six scalar equations:

$$\boldsymbol{\phi} = \begin{Bmatrix} \mathbf{r}^a + \mathbf{A}^a {}^a\mathbf{r}^P - \mathbf{r}^b - \mathbf{A}^b {}^b\mathbf{r}^P \\ \mathbf{A}^a {}^a\mathbf{u} - \mathbf{A}^b {}^b\mathbf{u} \end{Bmatrix} = 0 \tag{11.72}$$

where only two of the last three equations are independent. The matrices $\mathbf{A}^a$ and $\mathbf{A}^b$ are (3x3) orthogonal rotation matrices given by

$$\mathbf{A}^a = \left[\mathbf{m}^a \wedge \mathbf{n}^a \middle| \mathbf{m}^a \middle| \mathbf{n}^a \right] \quad \text{and} \quad \mathbf{A}^b = \left[\mathbf{m}^b \wedge \mathbf{n}^b \middle| \mathbf{m}^b \middle| \mathbf{n}^b \right] \tag{11.73}$$

where the vertical bars denote the separation between columns. The values of ${}^a\mathbf{r}^P$, ${}^b\mathbf{r}^P$, ${}^a\mathbf{u}$, and ${}^b\mathbf{u}$ are the coordinates of point P and the components of vector $\mathbf{u}$ expressed in frames a and b, respectively.

In the previous example, the joint is linking two beams, but the joint could also be thought as linking a beam and a rigid body or a beam and a flexible body with assumed deformation modes. The joint constraints would be developed in the same way, but different position variables would be used for one of the bodies.

11.3.6 Governing Equations of Motion

Once more the equations of motion can be derived using any of the methods seen in Chapter 4. Here, the Lagrange multipliers method will be used again. The Lagrangian function L can be written as

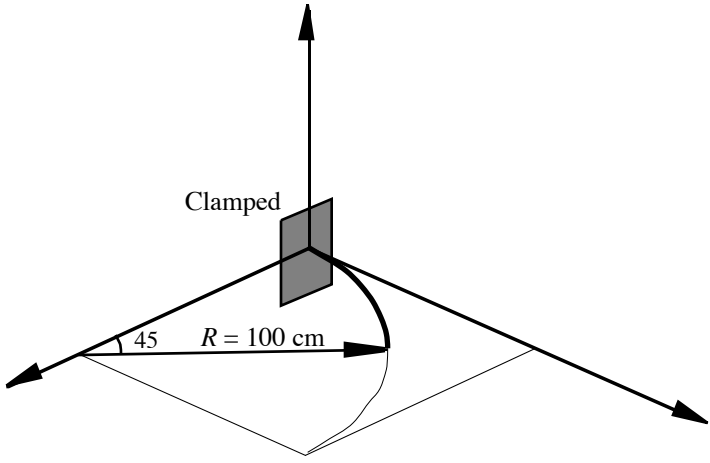

Figure 11.12. Cantilever beam 45-degree bend.

$$L = T - \Pi + \mathbf{\Phi}^{\mathrm{T}}\,\boldsymbol{\lambda} \tag{11.74}$$

where $\mathbf{\Phi}$ contains the constraints that arise from the unit norm and orthogonality condition that the nodal variables have to satisfy at the nodes and from the kinematic constraints imposed at the joints. Vector $\boldsymbol{\lambda}$ contains the Lagrange multipliers corresponding to the constraints.

The application of the Lagrange's equations leads to

$$\mathbf{M}\,\ddot{\mathbf{q}} + \mathbf{\Phi}_{\mathbf{q}}^{\mathrm{T}}\,\boldsymbol{\lambda} = \mathbf{Q} - \mathbf{F} \tag{11.75}$$

where $\mathbf{M}$ is the mass matrix obtained by assembling the mass matrices $\mathbf{M}^{\mathrm{e}}$ of each element, $\mathbf{\Phi}_{\mathbf{q}}$ the Jacobian matrix of the constraint equations, $\mathbf{Q}$ the vector of generalized external forces, and $\mathbf{F}$ the elastic forces. The elastic forces are obtained by differentiating equation (11.65) with respect to $\mathbf{q}^{\mathrm{e}}$, giving

$$\begin{aligned}\mathbf{F}^{\mathrm{e}} = \int_0^L \Big[& E\,A\,\Gamma_1\,\mathbf{G}^1 + E\,I_2\,\Gamma_2\,\mathbf{G}^2 + E\,I_3\,\Gamma_3\,\mathbf{G}^3 + G\,A_{\mathrm{s}2}\,\Gamma_4\,\mathbf{G}^4 + \\ & + G\,A_{\mathrm{s}3}\,\Gamma_5\,\mathbf{G}^5 + G\,I_{\mathrm{p}}\,\Gamma_6\,\mathbf{G}^6 \Big]\, dX_1\,\mathbf{q}^{\mathrm{e}}\end{aligned} \tag{11.76}$$

The matrices $\mathbf{G}^{\mathrm{i}}$ are very sparse, and consequently the multiplications by $\mathbf{q}^{\mathrm{e}}$ can be carried out analytically with very few arithmetic operations.

11.3.7 Numerical Examples

In this section, the results obtained in three examples are presented in order to test both the accuracy of the present beam finite element and the numerical inte-

Table 11.1. Tip displacement (cm) in the cantilever 45-degree bend.

	f = 300 Kg			f = 450 Kg			f = 600 Kg		
	x_1	x_2	x_3	x_1	x_2	x_3	x_1	x_2	x_3
Present method	22.14	58.66	40.65	18.23	51.84	49.31	15.26	46.48	54.54
Cardona (1989)	22.14	58.64	40.35	18.38	52.11	48.59	15.55	47.04	53.50
Simo (1986)	22.33	58.84	40.08	18.62	52.32	48.39	15.79	47.23	53.37
Bathe and B. (1979)	22.50	59.20	39.50	-	-	-	15.90	47.20	53.40
Crisfield (1990)	22.16	58.53	40.53	18.43	51.93	48.79	15.61	46.48	53.71

gration procedure. In all cases, the penalty matrix $\boldsymbol{\alpha}$ was taken as $\alpha\mathbf{I}$, and the value of the penalty factor α was taken as 10^6 times the largest term appearing in the tangent stiffness matrix $\mathbf{H}_{\mathbf{qF}}$ obtained through differentiation of equation (11.76). No attempt was made to optimize the value of the penalty factor. It was found that the iteration process converged in few iterations and that the constraint violation was kept small, roughly $\|\boldsymbol{\phi}\| < \alpha^{-1}$. The calculations were performed in a Silicon Graphics 4D/240 using only one processor. To avoid the *shear-locking*, reduced integration has been used for the shear terms.

Example 11.2

The 45-degree bend cantilever beam shown in Figure 11.12 of radius equal to 100 *cm* shall be considered. It is located in a horizontal plane and a vertical static load f will be considered acting at the tip. The beam has a unit square cross section and $E = G = 10^7$ Kg/cm^2. It is discretized using eight linear straight elements.

In Table 11.1, the three coordinates of the tip in the deformed position are presented for three different values of the force. The values obtained with the finite element developed in this chapter are compared to the values obtained previously by Cardona (1989), Simo (1986), Bathe and Bolourchi (1979), and Crisfield (1990). The total load is applied in six equally-spaced load increments.

It is worth noting that the tip displacements are of the same order of magnitude as the length of the beam, which is 78.54 cm. Therefore, the behavior of the beam is totally nonlinear, with finite displacements which could not be studied using a mode superposition method. As the value of the load increases the solution provided by the proposed method gives larger displacements than the other formulations. This is because the interpolation in each finite element, as discussed in Section 11.3.2, does not satisfy the orthogonality condition for variables $(\mathbf{m}, \mathbf{n})$. This static example is an extreme one, and it has been presented to prove that this assumption is valid. In fact, the maximum discrepancy between the results presented in Table 11.1 for the different methods is about two per cent.

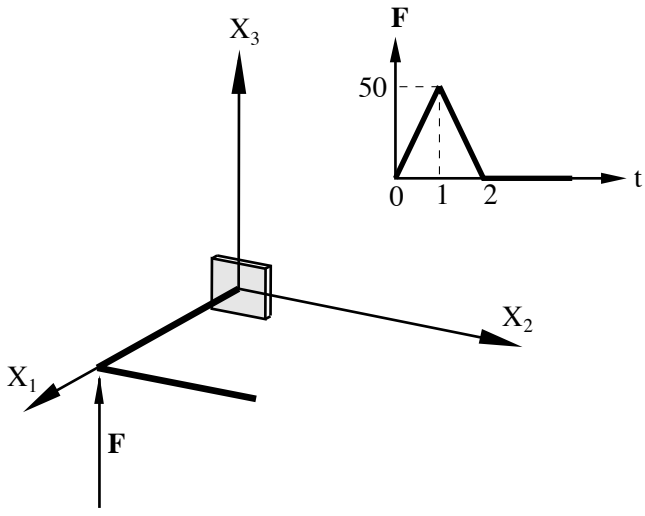

Figure 11.13. Right-angle cantilever beam.

Example 11.3

This example, a right-angle cantilever beam, was first proposed by Simo and Vu-Quoc (1988) and solved with quadratic elements. Later, it was solved by Cardona (1989) using linear elements with a very similar formulation as the previous one. The problem consists of a right-angle cantilever beam composed of two straight parts of length L=10, each, as shown in Figure 11.13.

The physical characteristics of the beam are not realistic, but they are useful to test the accuracy of the method in a dynamic simulation when large relative displacements appear. Their values, using the notation in Simo and Vu-Quoc (1988), are given below:

$$GA = EA = 10^6$$
$$EI_2 = EI_3 = GI_p = 10^3$$
$$A_\rho = 1$$
$$I_{\rho 1} = 2I_{\rho 2} = 2I_{\rho 3} = 20$$

There is a dynamic vertical load F acting at the elbow with a triangular variation law. The load acts for 2 sec and reaches a peak of F_{max}=50 at t=1 sec, as can be seen in Figure 11.13. The problem has been solved with two different discretizations using four and eight linear elements. The total simulation time is 30 sec. In Figures 11.14 and 11.15, the vertical displacements of the elbow and the tip obtained with four and eight elements are plotted. The agreement of this dynamic response compared to Simo and Vu-Quoc (1988) and Cardona (1989) is poor for the four elements discretization, but it is good when eight elements are used.

The results were obtained using a constant step size of 0.125 sec. The average number of iterations in the Newton-Raphson procedure was three. The *CPU* times were 20.6 sec for the four elements discretization and 44.4 sec for the eight elements discretization .

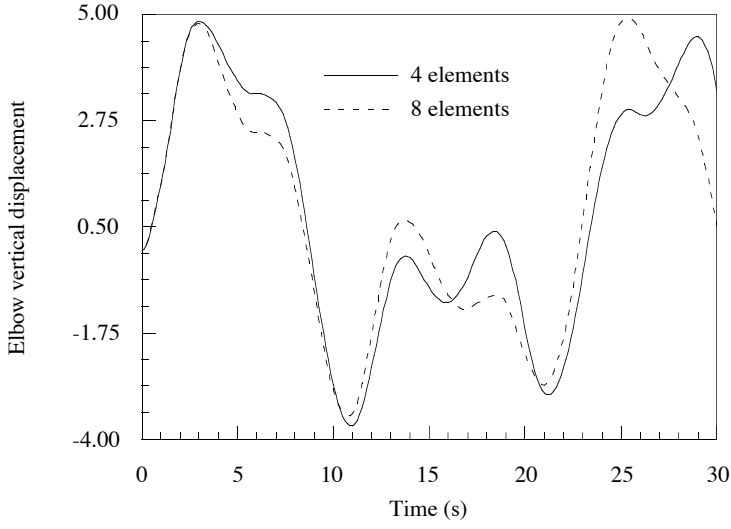

Figure 11.14. Elbow vertical displacement using four and eight finite elements.

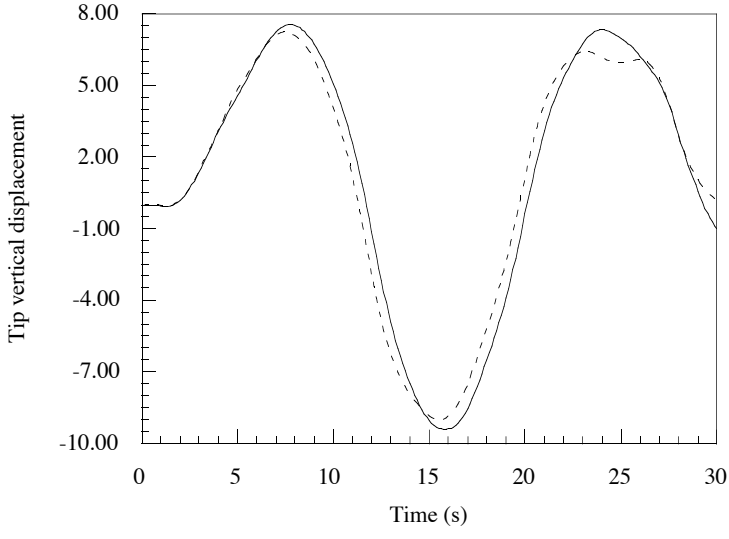

Figure 11.15. Tip vertical displacement using four and eight finite elements.

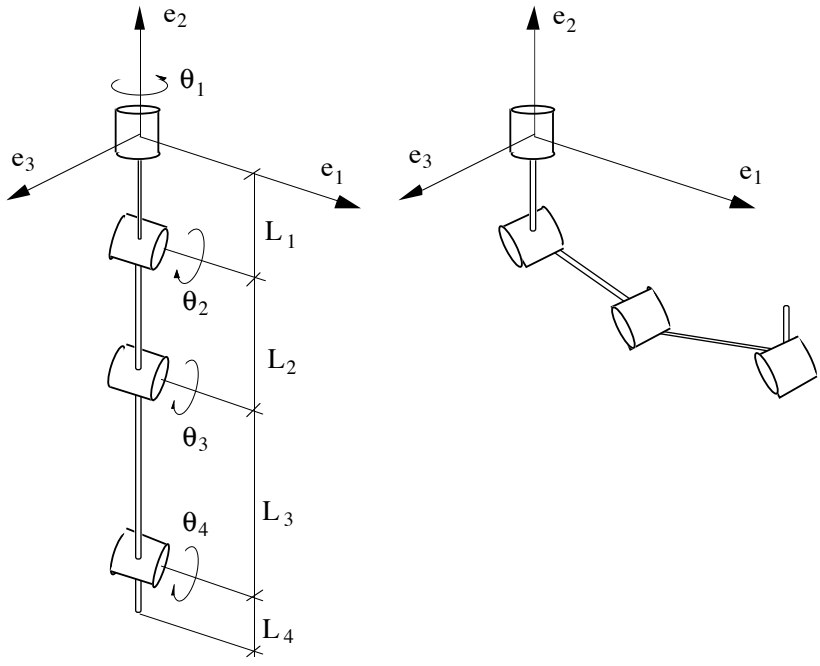

Figure 11.16. Spatial manipulator with two flexible links.

Example 11.4

A flexible spatial manipulator composed of two rigid and two flexible links is presented in Figure 11.16. Links 2 and 3 are flexible beams of tubular section. Each link is connected to the previous one through a revolute joint. At the midpoint of link 4 a lumped mass of 200 Kg has been attached to represent a load. The geometric and material properties of the links are:

$L_1 = 0.3$ m
$L_2 = 4.0$ m
$L_3 = 5.0$ m
$L_4 = 0.5$ m
$E = 6895\ 10^7$ N/m^2
$\rho = 2699$ Kg/m^3

Inner radius of the cross section for links 2 and 3.
$r_i = 0.04$ m

Outer radius of the cross section for links 2 and 3.
$r_o = 0.05$ m

Links 1 and 4 have been modeled, respectively, with a single finite element of high-elasticity modulus, and links 2 and 3 have been modeled with four elements each. The simulation that has been carried out is based on a prescribed motion in each revolute joint that moves the manipulator from the initial configuration to the final one, both shown in Figure 11.16. The prescribed motion is such that

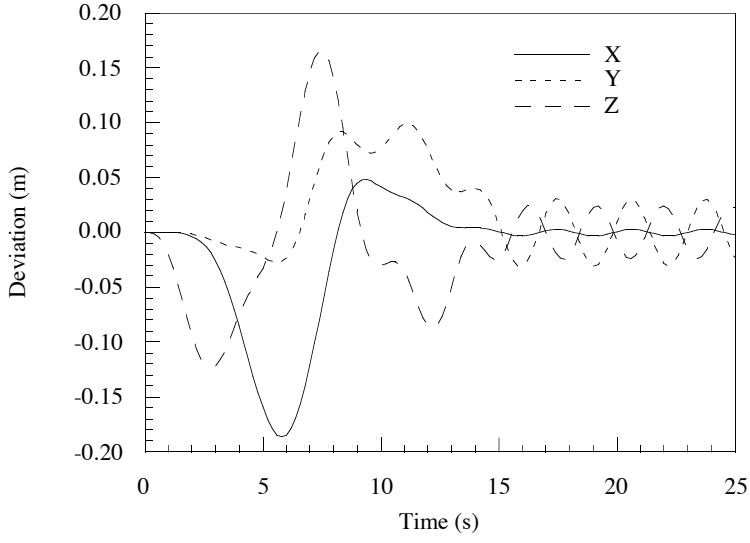

Figure 11.17. Tip deviations in the X, Y, and Z directions with respect to the rigid body trajectory.

there is a rotation of 90 degrees in joints 1 and 4 and a rotation of 45 degrees in joints 2 and 3. The variation law of each joint is the following:

$$\theta_1 = \theta_4 = \begin{cases} \dfrac{\pi}{2T_s}\left(t - \dfrac{T_s}{2\pi}\, sin\left(\dfrac{2\pi t}{T_s}\right)\right) & 0 \le t \le T_s \\ \dfrac{\pi}{2} & t \ge T_s \end{cases}$$

$$\theta_2 = \theta_3 = \begin{cases} \dfrac{\pi}{4T_s}\left(t - \dfrac{T_s}{2\pi}\, sin\left(\dfrac{2\pi t}{T_s}\right)\right) & 0 \le t \le T_s \\ \dfrac{\pi}{4} & t \ge T_s \end{cases}$$

The total simulation time is 25 sec, and T_S was taken to be 15 sec. Figure 11.17 illustrates the three (X,Y,Z) components of the tip deviation with respect to the nominal motion (that is, the trajectory obtained with all the links considered as rigid) as a function of time. The CPU time is 43.2 sec with a fixed step size of 0.2 sec and an average of 3.3 Newton-Raphson iterations per step.

References

Avello, A., "Dinámica de Mecanismos Flexibles con Coordenadas Cartesianas y Teoría de Grandes Deformaciones", Ph.D. Thesis, University of Navarre, San Sebastián, (1990).

Bathe, K.-J., *Finite Element Procedures in Engineering Analysis*, Prentice-Hall, (1982).

Bathe, K.-J. and Bolourchi, S., "Large Displacement Analysis of Three-Dimensional Beam Structures", *International Journal for Numerical Methods in Engineering*, Vol. 14, pp. 961-986, (1979).

Bayo, E. and Serna, M.A., "Penalty Formulations for the Dynamic Analysis of Elastic Mechanisms", *Journal of Mechanisms, Transmissions, and Automation in Design,* Vol. 111, pp.321-327, (1989).

Book, W.J., "Recursive Lagrangian Dynamics of Flexible Manipulator Arms", *International Journal of Robotics Research*, Vol. 3, pp. 87-101, (1984).

Cardona, A., "An Integrated Approach to Mechanism Analysis", Ph.D. Thesis, Université de Liége, Belgium, (1989).

Changizi, K. and Shabana, A.A., "A Recursive Formulation for the Dynamic Analysis of Open-Loop Deformable Multibody Systems", *ASME Journal of Applied Mechanics*, Vol. 55, pp. 687-693, (1988).

Craig, R.R., *Structural Dynamics*, Wiley, (1981).

Crisfield, M.A., "A Consistent Co-Rotational Formulation for Non-Linear, Three Dimensional, Beam-Elements", *Computer Methods in Applied Mechanics and Engineering*, Vol. 81, pp. 131-150, (1990).

Erdman, E.G. and Sandor, G.N., "Kineto-Elastodynamics – A Review of the State of the Art Trends", *Mechanism and Machine Theory*, Vol. 7, pp. 19-33, (1972).

Erdman, A.G. and Sung, C.K., "A Survey of Finite Element Techniques for Mechanism Design", *Mechanism and Machine Theory*, Vol. 21, pp. 351-359, (1986).

Hurty, W.C., "Dynamic Analysis of Structural Systems Using Component Modes", *AIAA Journal*, Vol. 3, pp. 678-685, (1965).

Kane T.R., Ryan R.R., and Banerjee, A.K., "Dynamics of a Cantilever Beam Attached to a Moving Base", *AIAA Journal of Guidance, Control, and Dynamics*, Vol. 10, pp. 139-151, (1987).

Kim, S.-S. and Haug, E.J., "A Recursive Formulation for Flexible Multibody Dynamics. Part I: Open-Loop Systems", *Computer Methods in Applied Mechanics and Engineering*, Vol. 71, pp. 293-314, (1988).

Kim, S.-S. and Haug, E.J., "A Recursive Formulation for Flexible Multibody Dynamics. Part II: Closed-Loop Systems", *Computer Methods in Applied Mechanics and Engineering*, Vol. 74, pp. 251-269, (1989).

Lowen, G.G. and Jandrasits, W.G., "Survey of Investigations into the Dynamic Behavior of Mechanisms Containing Links with Distributed Mass and Elasticity", *Mechanism and Machine Theory*, Vol. 7, pp. 3-17, (1972).

Lowen, G.G. and Chassapis, C., "The Elastic Behavior of Linkages: An Update", *Mechanism and Machine Theory*, Vol. 21, pp. 33-42, (1986).

Malvern, L.E., "*Introduction to the Mechanics of a Continuous Medium*", Prentice-Hall, (1969).

Midha, A., Erdman, A.G., and Frohrib, D.A., "Finite Element Approach to Mathematical Modelling of High-Speed Elastic Linkages", *Mechanism and Machine Theory*, Vol. 13, pp. 603-618, (1978).

Naganathan, G. and Soni, A.H., "Coupling Effects of Kinematics and Flexibility in Manipulators", *International Journal of Robotics Research*, Vol. 6, pp. 75-85, (1987).

Shabana, A.A., *Dynamics of Multibody Systems*, Wiley, (1989).

Shabana, A.A. and Wehage, R.A., "A Coordinate Reduction Technique for Transient Analysis of Spatial Substructures with Large Angular Rotations", *Journal of Structural Mechanics*, Vol. 11, pp. 401-431, (1983).

Serna, M.A. and Bayo, E., "A Simple and Efficient Computational Approach for the Forward Dynamics of Elastic Robots", *Journal of Robotic Systems*, Vol. 6, pp. 363-382, (1989).

Simo, J.C., "A Three-Dimensional Finite-Strain Rod Model. Part II: Computational Aspects", *Computer Methods in Applied Mechanics and Engineering*, Vol. 58, pp. 79-116, (1986).

Simo, J.C. and Vu-Quoc L., "On the Dynamics of Flexible Beams Under Large Overall Motions – The Planar Case: Part I", *ASME Journal of Applied Mechanics*, Vol. 53, pp. 849-854, (1986).

Simo, J.C. and Vu-Quoc L., "The Role of Non-Linear Theories in Transient Dynamic Analysis of Flexible Structures", *Journal of Sound and Vibration*, Vol. 119, pp. 487-508, (1987).

Simo, J.C. and Vu-Quoc L., "On the Dynamics of Space Rods Undergoing Large Overall Motions", *Computer Methods in Applied Mechanics and Engineering*, Vol. 66, pp. 125-161, (1988).

Song, J.O. and Haug, E.J., "Dynamic Analysis of Planar Flexible Mechanisms", *Computer Methods in Applied Mechanics and Engineering*, Vol. 24, pp. 359-381, (1980).

Sunada, W. and Dubowsky, S., "The Application of Finite Element Methods to the Dynamic Analysis of Flexible Spatial and Coplanar Linkage Systems", *ASME Journal of Mechanisms, Transmissions, and Automation in Design,* Vol. 103, pp. 643-651, (1981).

Vukasovic, N., Celigüeta, J.T. ,García de Jalón, J., and Bayo, E., "Flexible Multibody Dynamics Based on a Fully Cartesian System of Support Coordinates", *ASME Journal of Mechanical Design*, Vol. 115, pp. 294-299, (1993).

Winfrey, R.C., "Elastic Link Mechanism Dynamics", *ASME Journal of Engineering for Industry*, Vol. 93, pp. 268-272, (1971).